

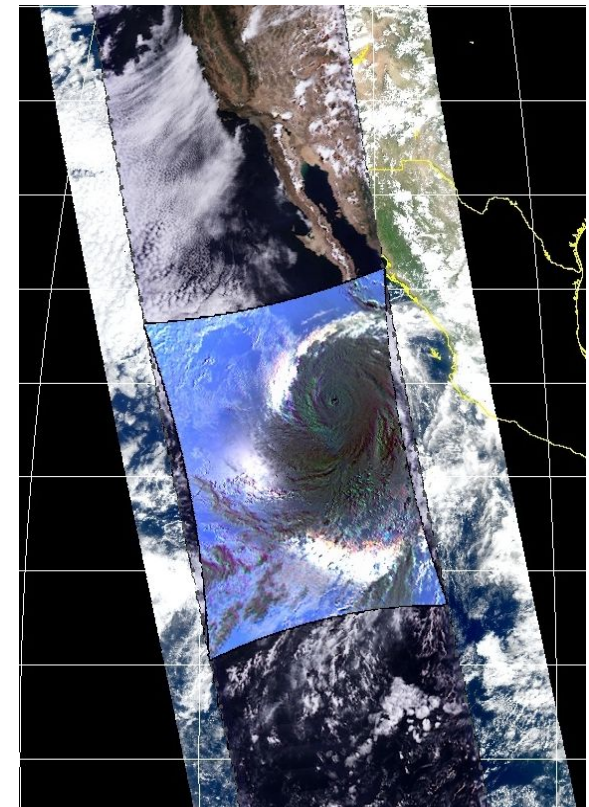
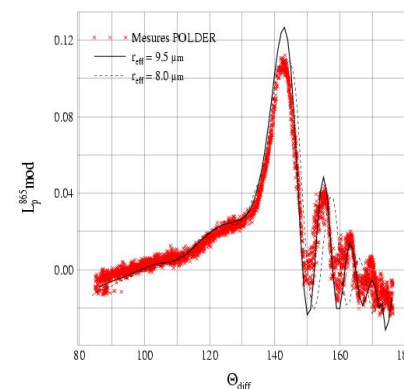
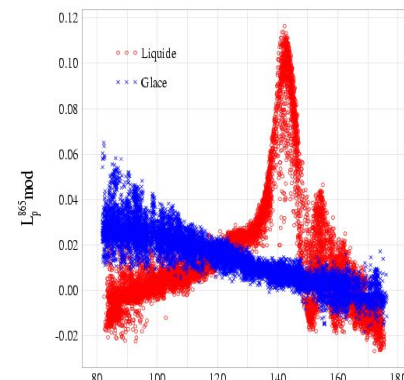
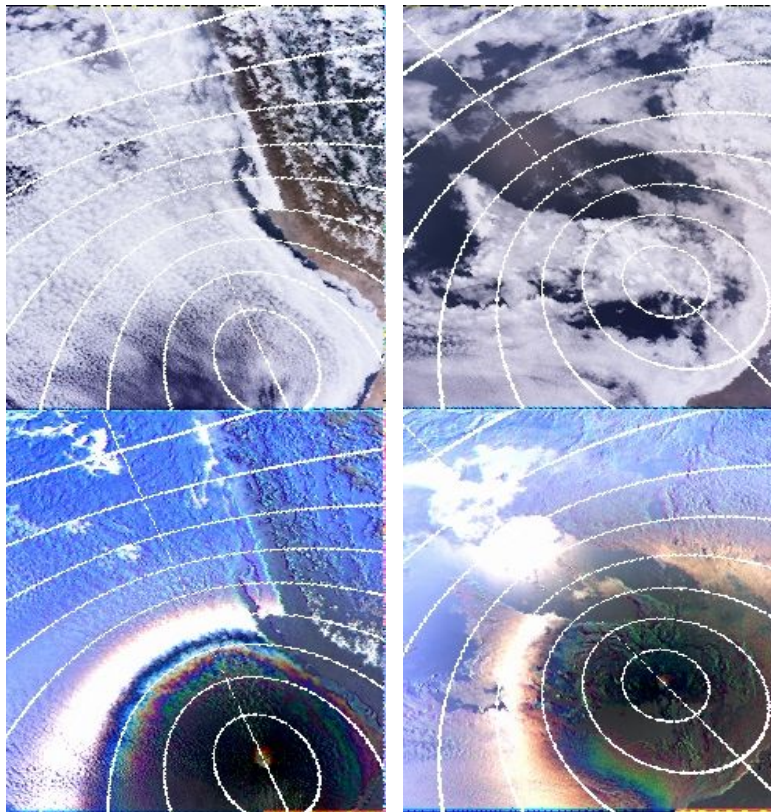
Clouds and aerosols remote sensing from POLDER to 3MI-EPS/SG

What polarization tells us ... and what it doesn't.

Prof. Jérôme Riedi

Laboratoire d'Optique Atmosphérique

University of Lille 1 - Science and Technology - FRANCE



OUTLINE

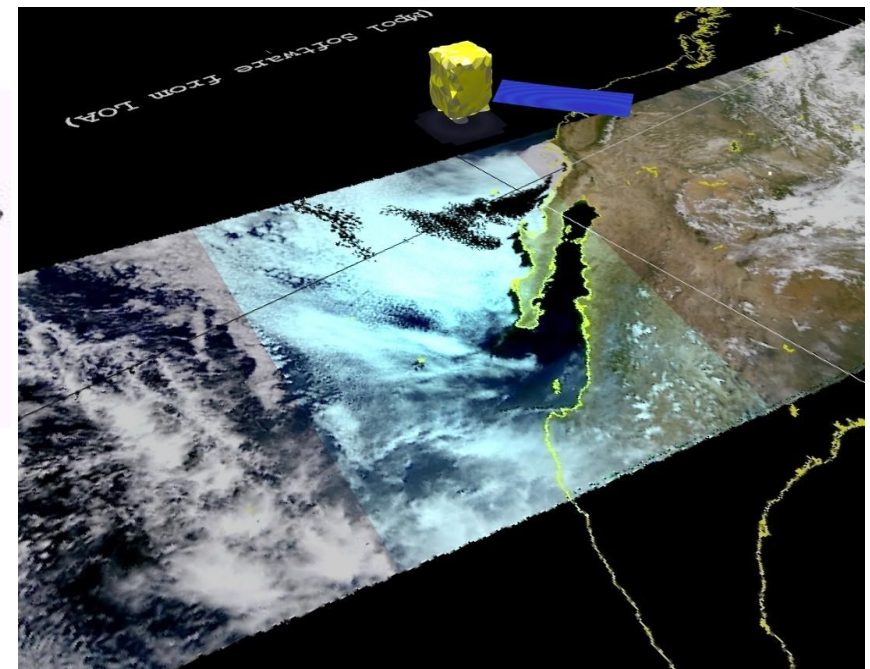
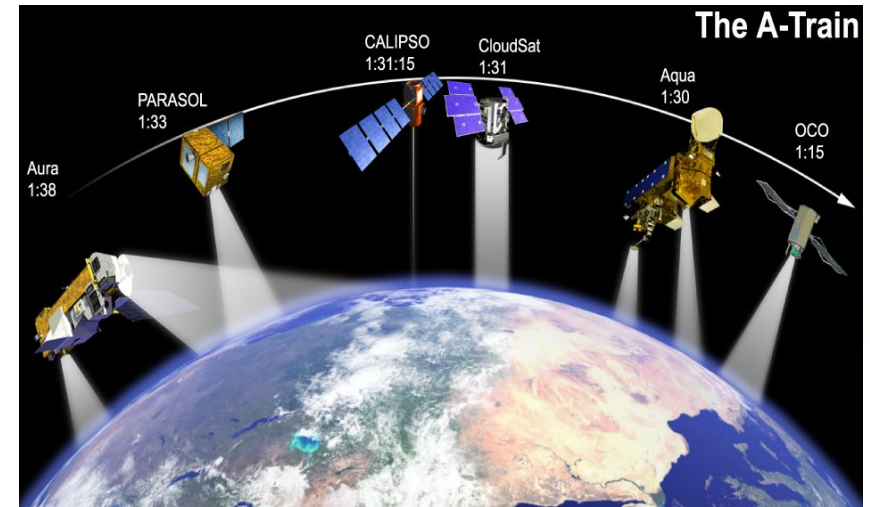
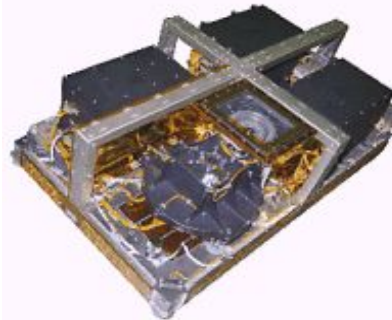
- What this talk is about :
 - POLDER measurement of polarized reflected sunlight
 - Cloud remote sensing from polarization multiangle measurements
 - Cloud microphysics (phase, shape, size distribution)
 - What is currently possible with multiangle polarization
 - What we can not or should not do with polarization
 - What polarization tells us about aerosols thanks to clouds
 - What's next ? 3MI on EPS-SG
- What it is not about : active remote sensing (lidar, radar)



Context & Instrumental Background

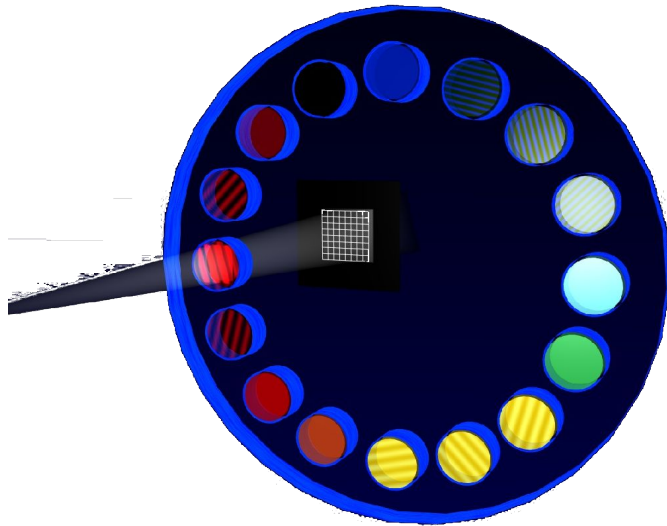


- CNES/LOA instrument,
 - POLDER1/ADEOS1 (1996-1997)
 - POLDER2/ADEOS2 (2003)
 - POLDER3/Parasol launched Dec. 2004
~ 705 km polar orbits, ascending (13:30 a.m.)
mission terminated in December 2014
- Sensor Characteristics (POLDER3)
 - 10 spectral bands ranging from 0.443 to 1.020 μm
 - 3 polarised channels
 - Wide FOV CCD Camera with 1800 km swath width
 - +/- 43 degrees cross track
 - +/- 51degrees along track
- Multidirectionnal observations
(up to 16 directions)
- Spatial resolution : 6x7 km
- No onboard calibration system - Inflight vicarious calibration :
 - 2-3% absolute calibration accuracy
 - 1% interband - 0.1% interpixel over clouds

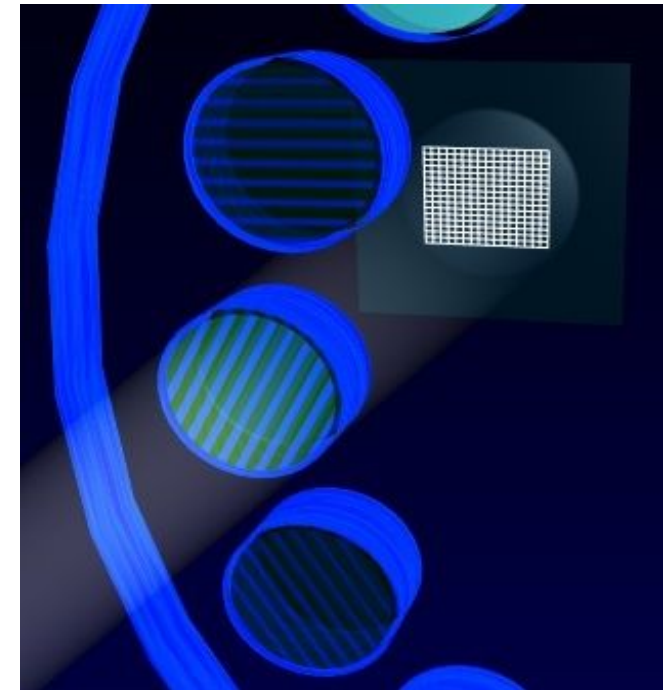




Context & Instrumental Background



A rotating filter wheel is used to acquire spectral and polarization measurements.

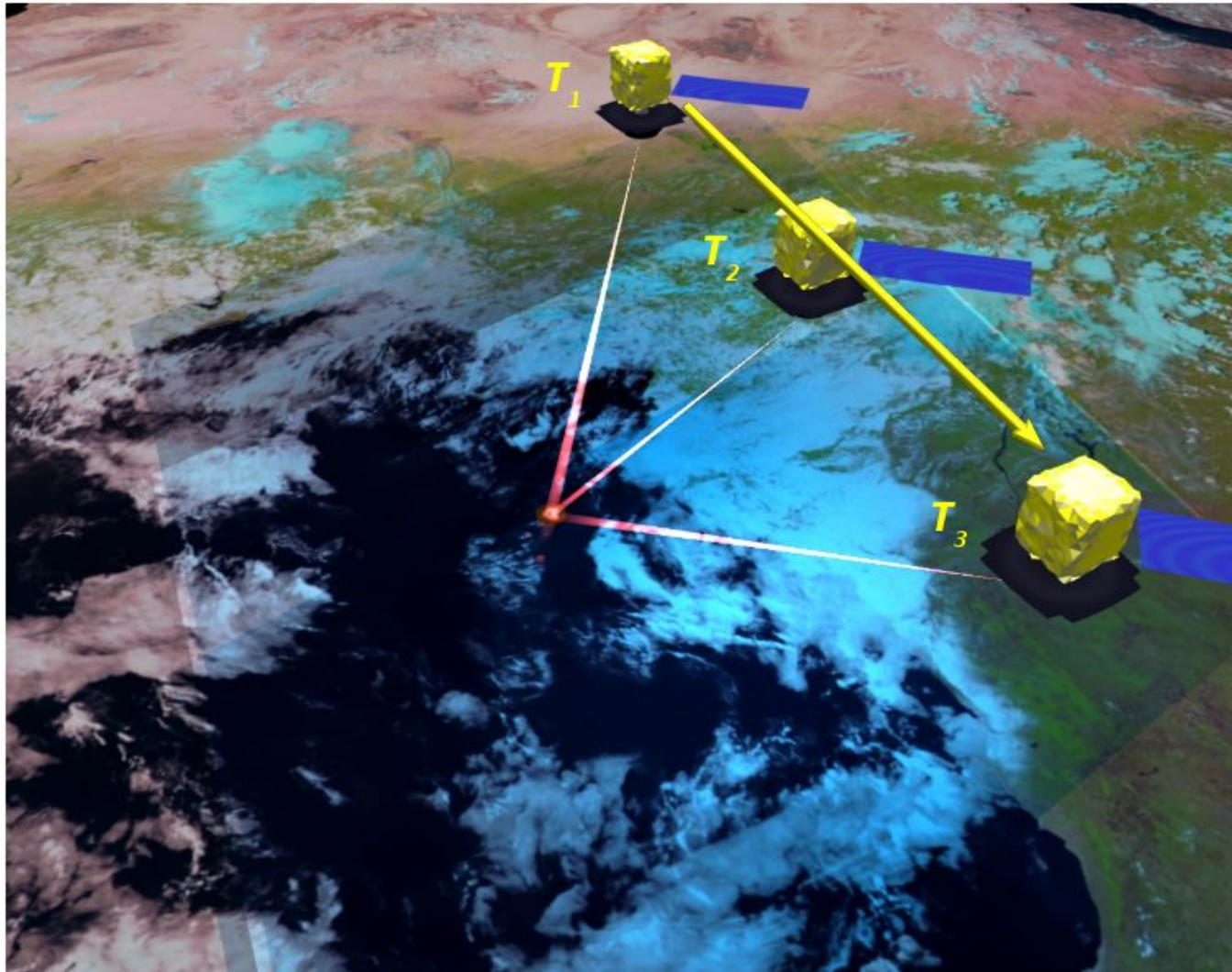


For each polarized channel 3 consecutive measurements S^1, S^2 and S^3 with polarizers oriented at $0, +/- 60$ degrees are used to retrieve the I, Q and U Stokes parameters (V is assumed to be 0 and not retrieved).
For each pixel i, j of the CCD array and for $\alpha = 60^\circ$:

$$\begin{bmatrix} S_{ij}^1 \\ S_{ij}^2 \\ S_{ij}^3 \end{bmatrix} = A \cdot \begin{bmatrix} 1 & -\frac{1}{2}(\cos 2\alpha - \sqrt{3} \sin 2\alpha) & -\frac{1}{2}(\sin 2\alpha + \sqrt{3} \cos 2\alpha) \\ 1 & \cos 2\alpha & \sin 2\alpha \\ 1 & -\frac{1}{2}(\cos 2\alpha + \sqrt{3} \sin 2\alpha) & -\frac{1}{2}(\sin 2\alpha + \sqrt{3} \cos 2\alpha) \end{bmatrix} \cdot \begin{bmatrix} L_{ij} \\ Q_{ij} \\ U_{ij} \end{bmatrix}$$

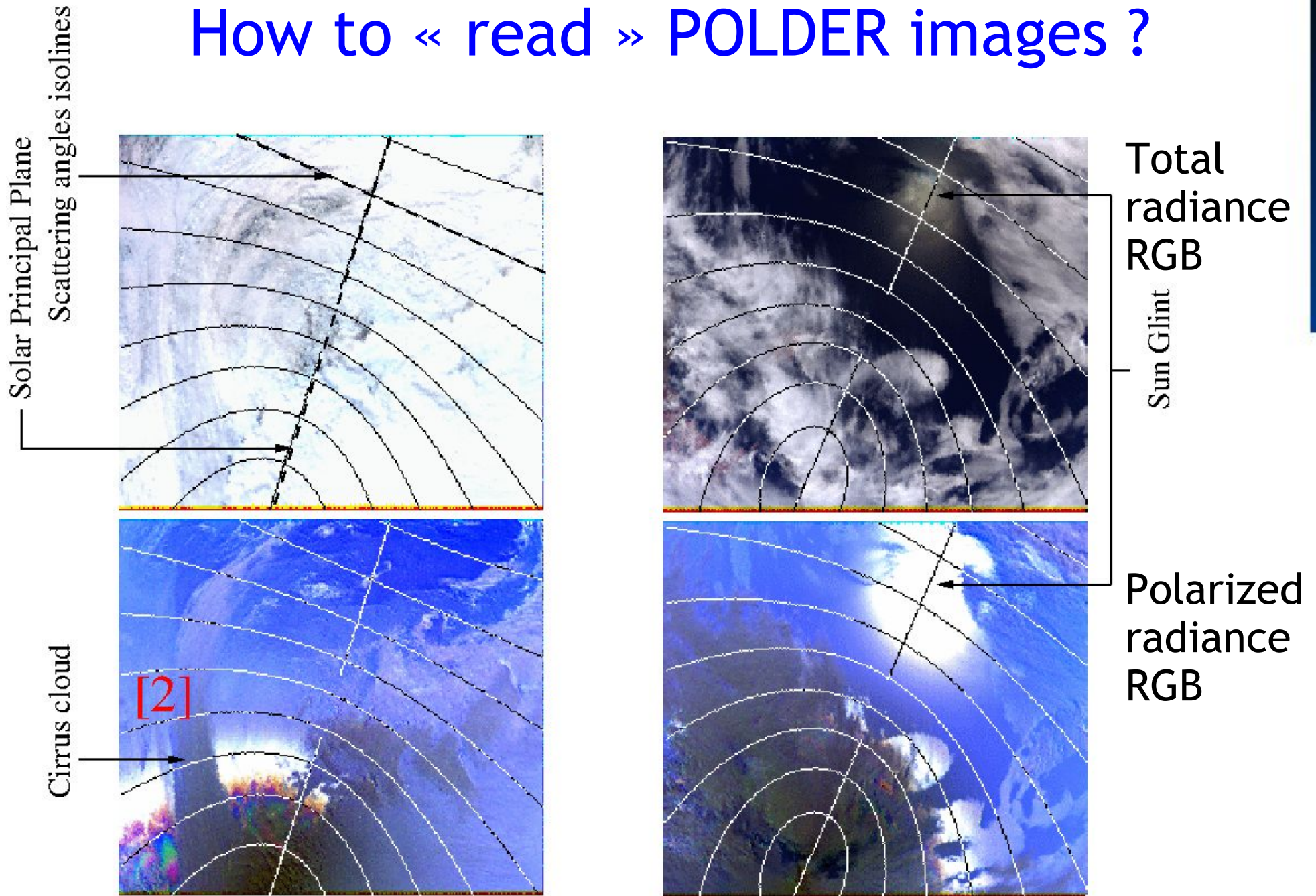


Context & Instrumental Background



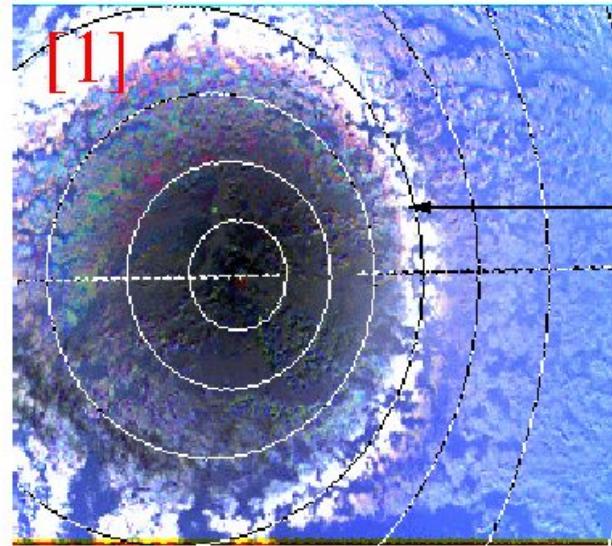
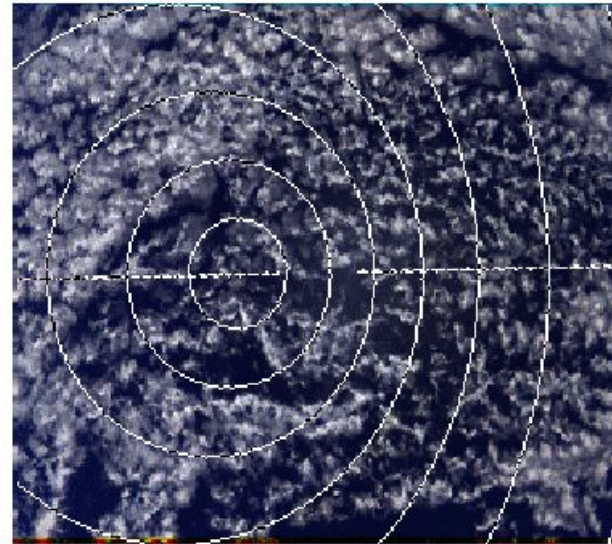
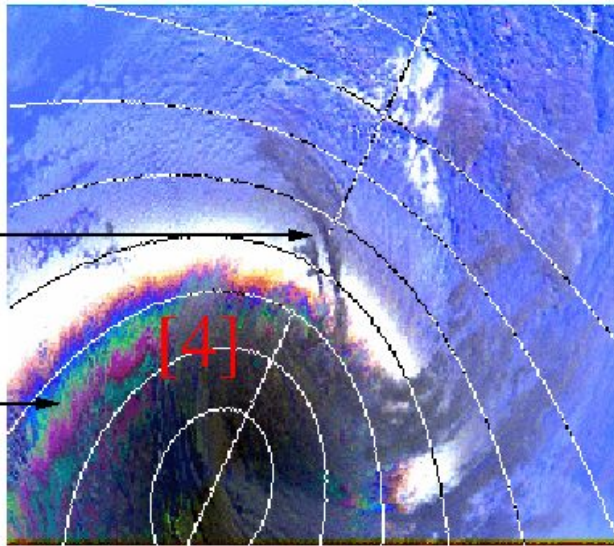
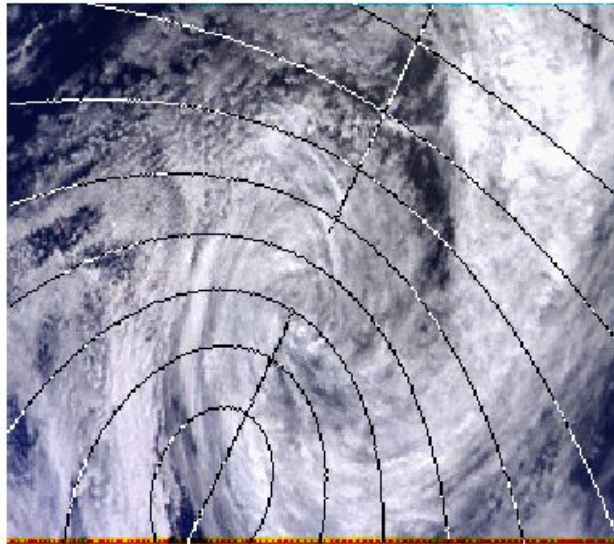
Multiangular sampling is achieved through multiple acquisition :
a given ground or atmosphere target remains in POLDER FOV

How to « read » POLDER images ?



How to « read » POLDER images ?

Irisation due to supernumerary bows
Cirrus masking liquid cloud bow



Total
radiance
RGB

Polarized
radiance
RGB

“Cloud bow” over broken liquid clouds field

A few things to keep in mind

- Polarization is produced by single scattering events but tend to vanish after a few multiple scattering
 - polarization signal tend to saturate for optical thickness > 2
 - must be careful when combining total radiance and polarized radiance measurements because they reach asymptotic regime for very different layer optical thickness
- Scattering properties and features of particles phase function are well preserved in polarized radiance
 - multiangle polarized reflectances act as fingerprints of scatterers

What we think we can do ...

Past Application to Clouds Remote Sensing

Polarization by clouds

D. Deirmendjian - Appl. Opt, 1964, J. E. Hansen - Journal of Atmos. Sci., 1971

Cloud phase

Goloub et al (2000), Riedi et al (2001), Riedi et al (2010)

Liquid Cloud Microphysics

Bréon and Goloub (1998), Bréon and Doutriaux (2005)

Ice Cloud Microphysics

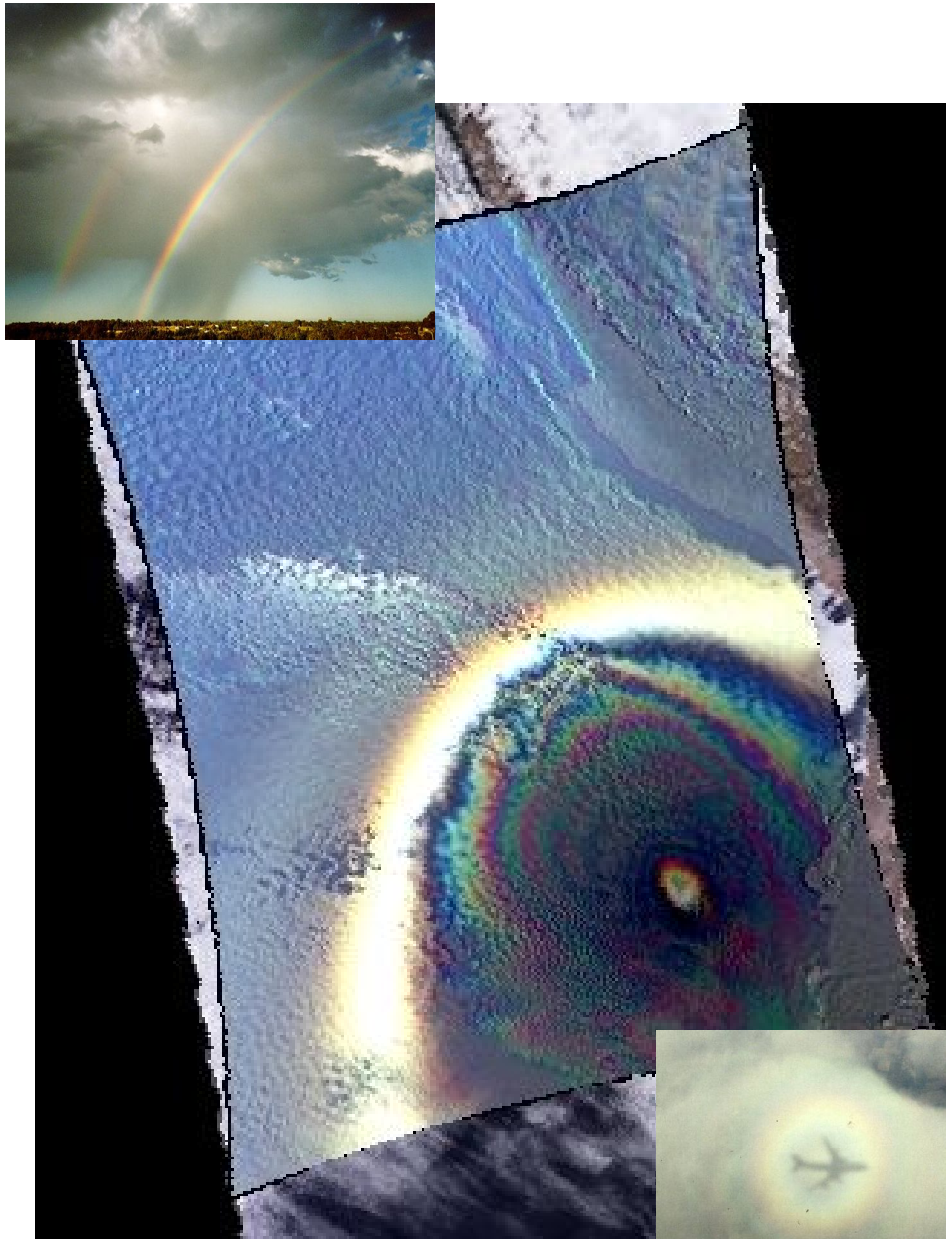
Chepfer et al (2001), Liou and Takano (2002), Baran and Labonnote (2006), Van Diedenhoven et al (2013), Cole et al (2014)

Oriented Particles Detection

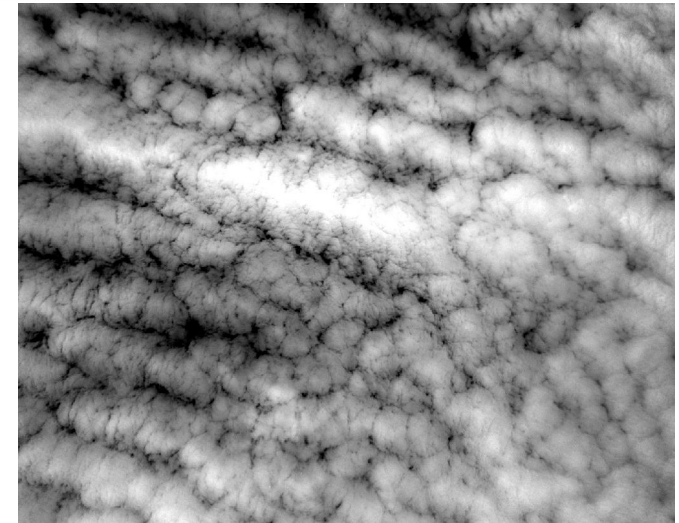
Chepfer et al (1999), Bréon and Dubrulle (2004), Noël et Chepfer (2004)

Cloud Top Pressure

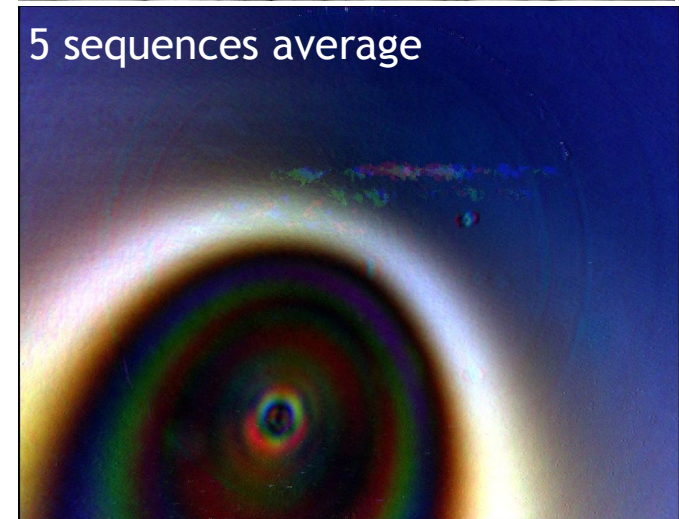
Buriez et al (1997), Vanbauce et al (2002)



POLDER3/PARASOL



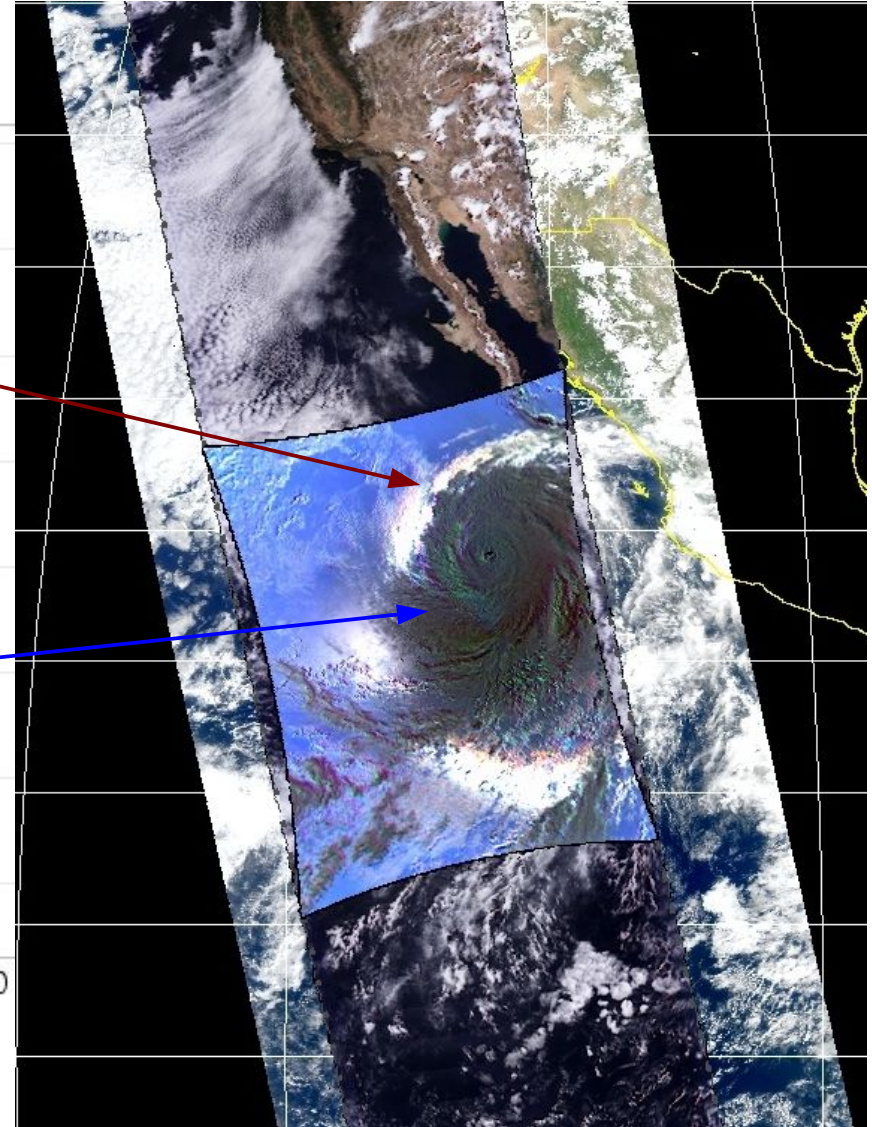
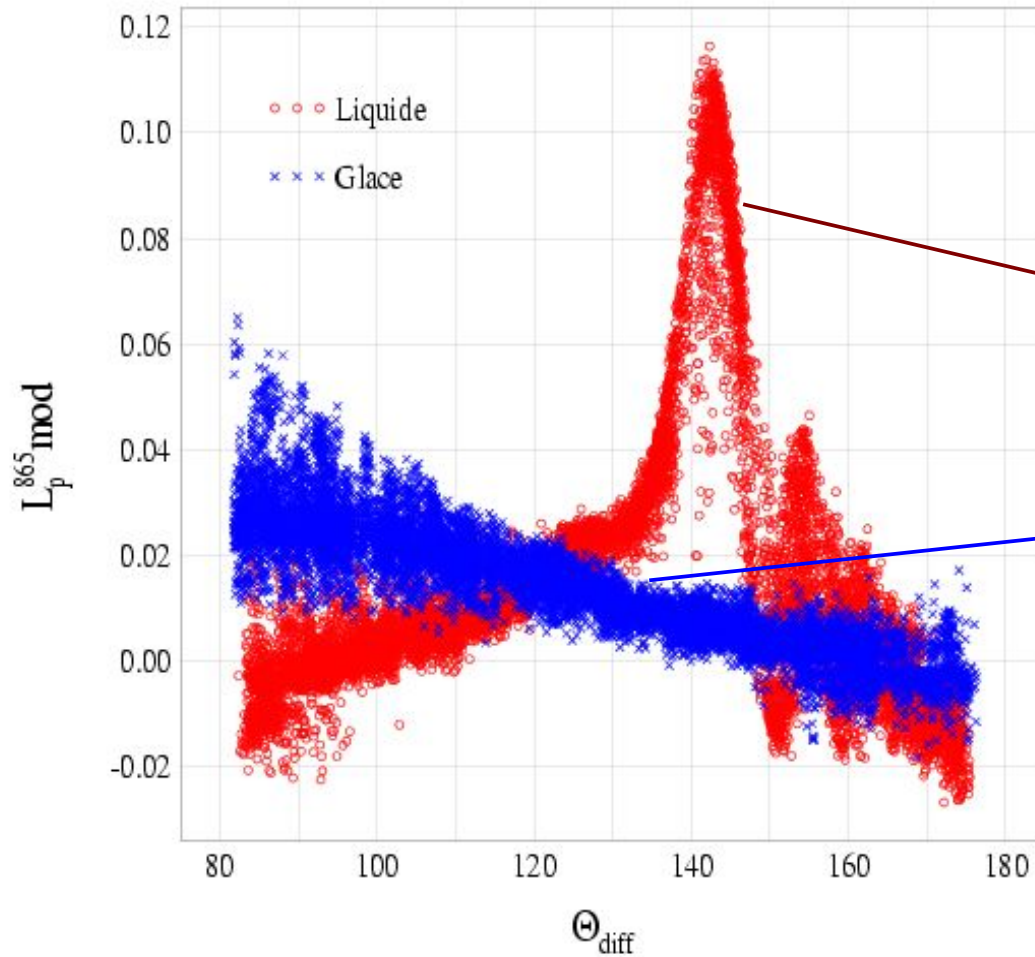
5 sequences average



OSIRIS : Airborne precursor for 3MI (EPS-SG)
Courtesy C. Cornet
See F. Auriol poster tonight

Cloud Top Thermodynamic Phase

Principle : particle shape discrimination spherical vs non sphe.



Goloub et al, Riedi et al

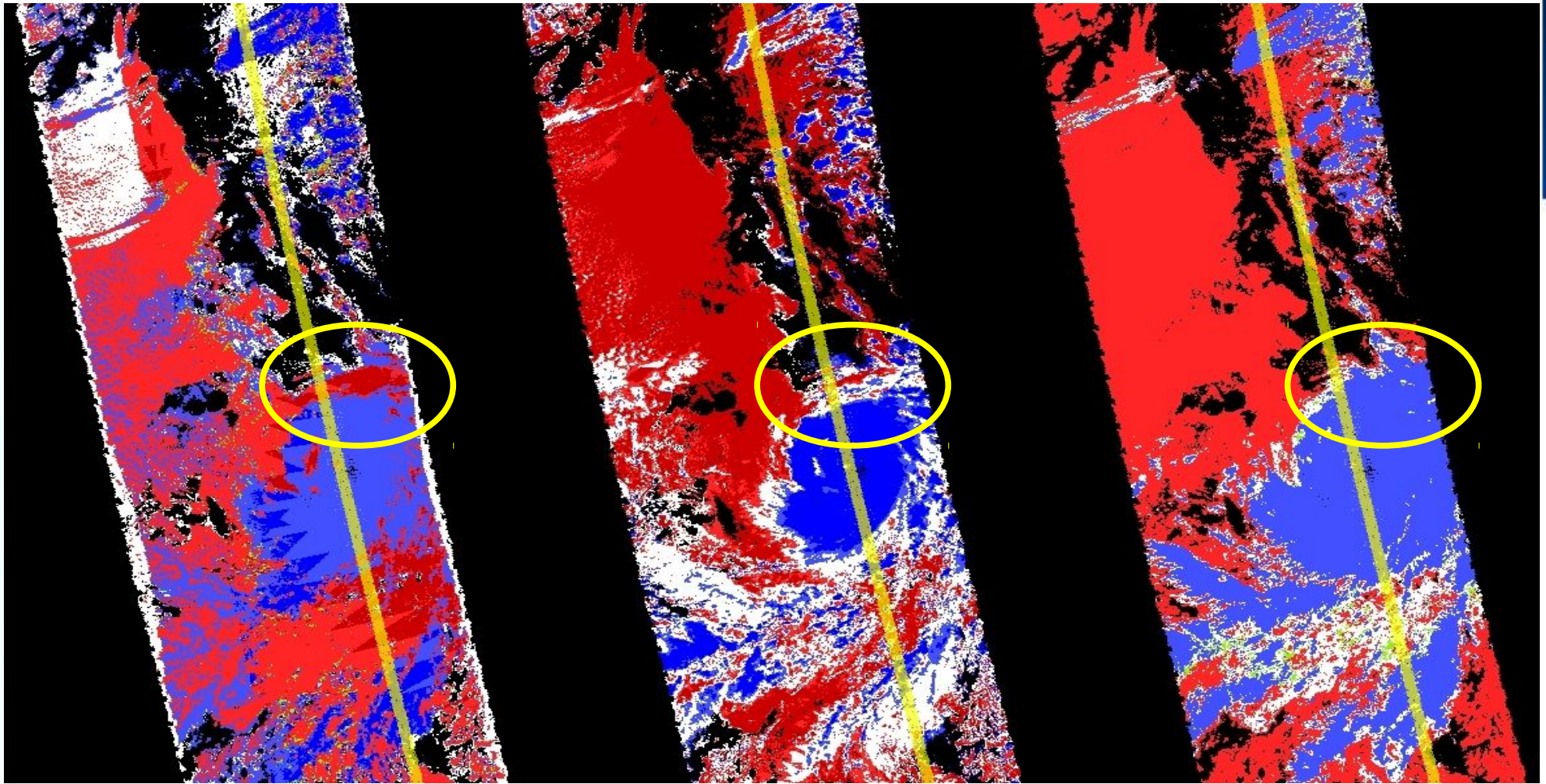
Cloud thermodynamic phase

Combination of information on particle shape and absorption properties
A-Train analysis : combining POLDER and MODIS to infer cloud phase

POLARIZATION

SWIR/VIS Ratio

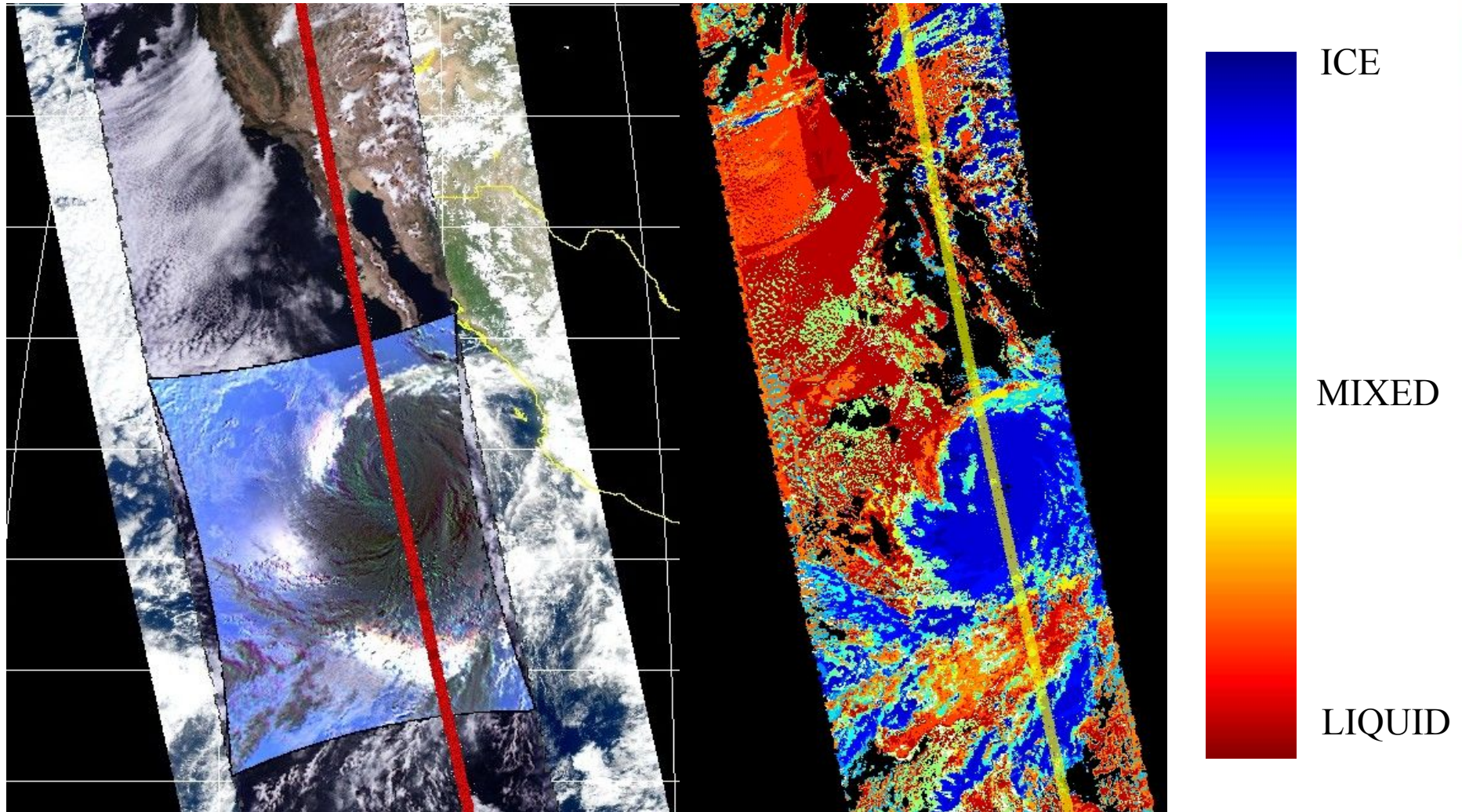
Thermal IR Bispectral



■ ■ ICE ■ UNKOWN ■ ■ LIQUID

Cloud thermodynamic phase

Combination of information on particle shape and absorption properties
A-Train analysis : combining POLDER and MODIS to infer cloud phase



Riedi et al, 2010 (ACP)

Science rationale : model ice crystal properties

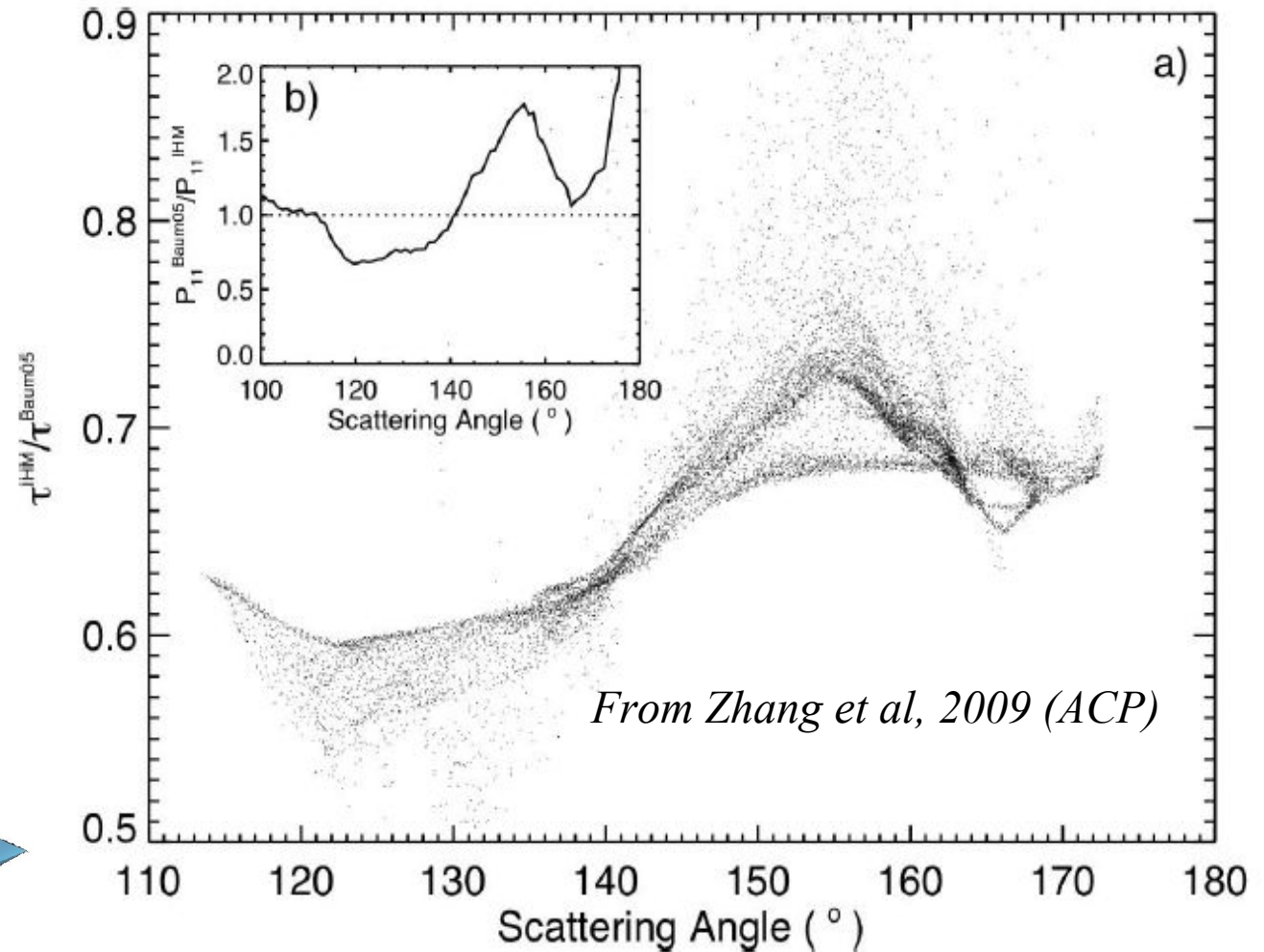
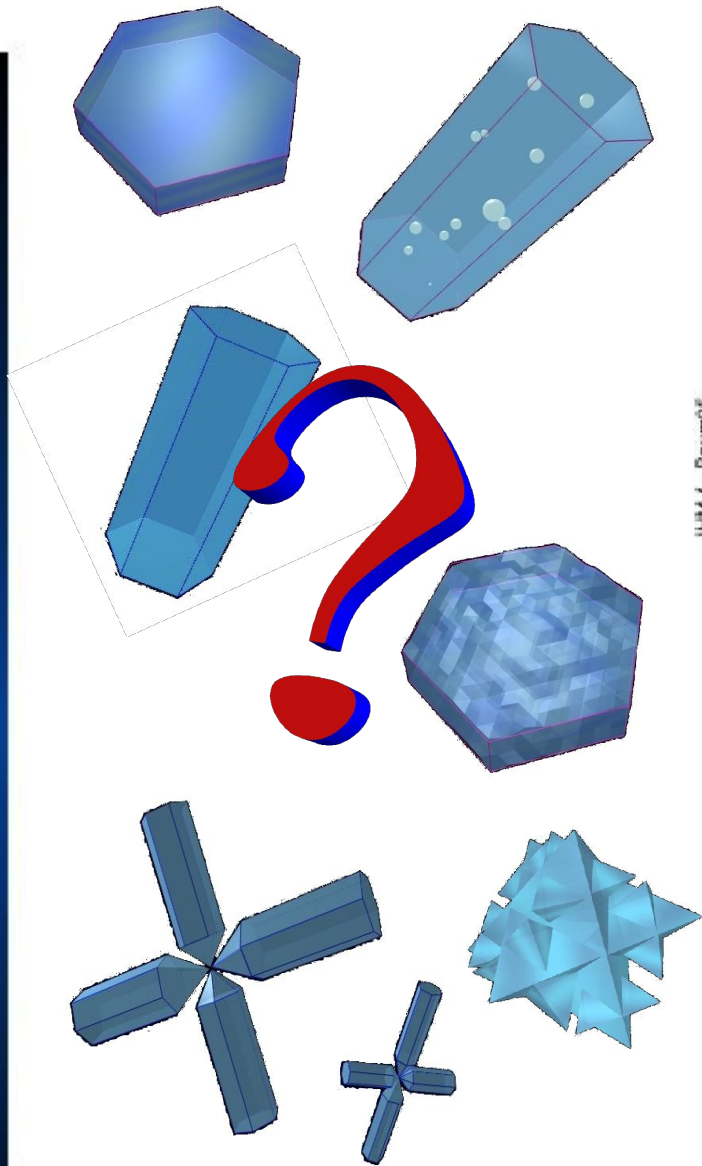
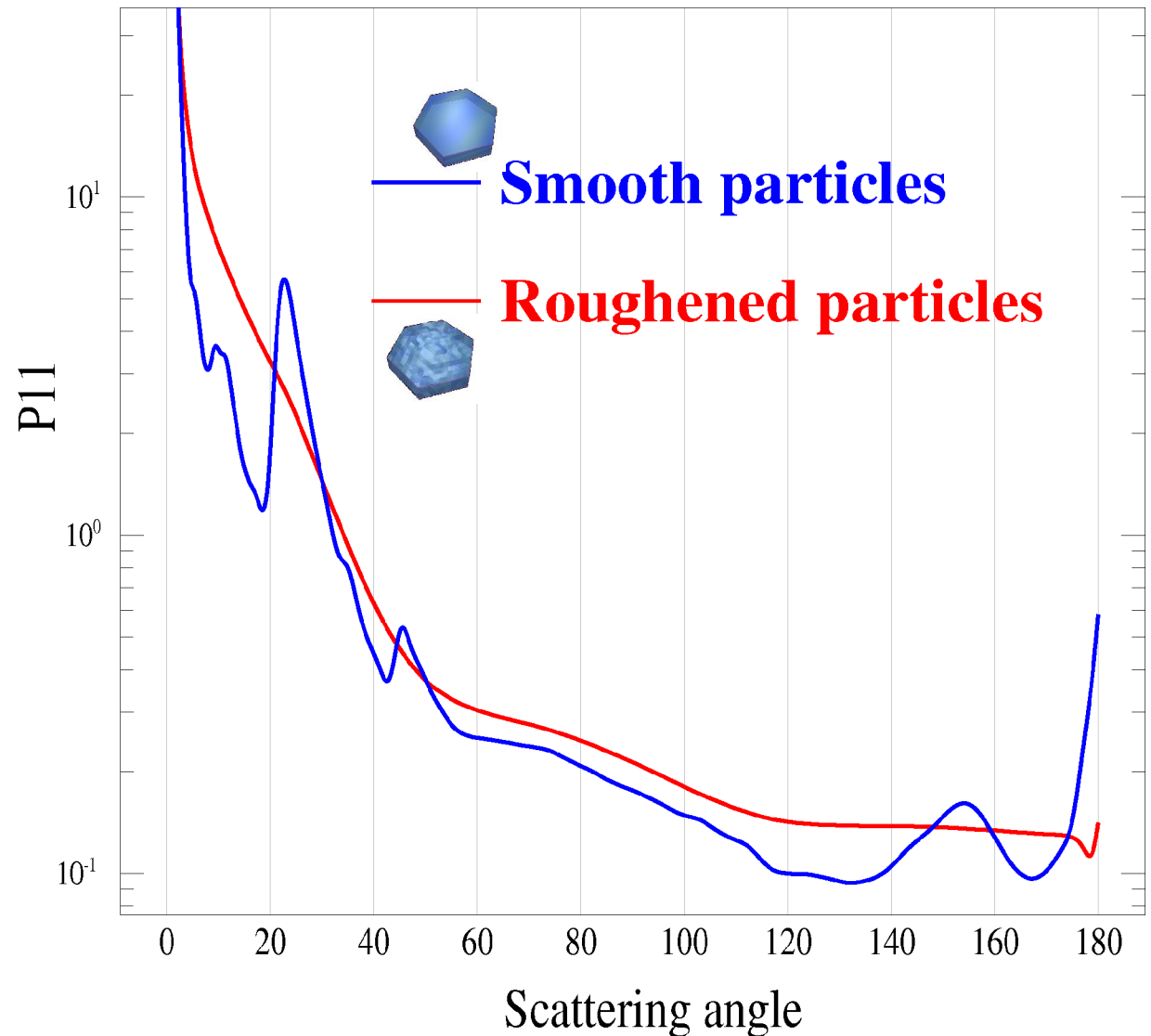


Fig. 7. The ratio of (a) $\tau_c^{IHM} / \tau_c^{Baum05}$ and (b) $P_{11}^{Baum05} / P_{11}^{IHM}$ as a function of scattering angle.

Angular reflectance features act as fingerprints of particle shapes

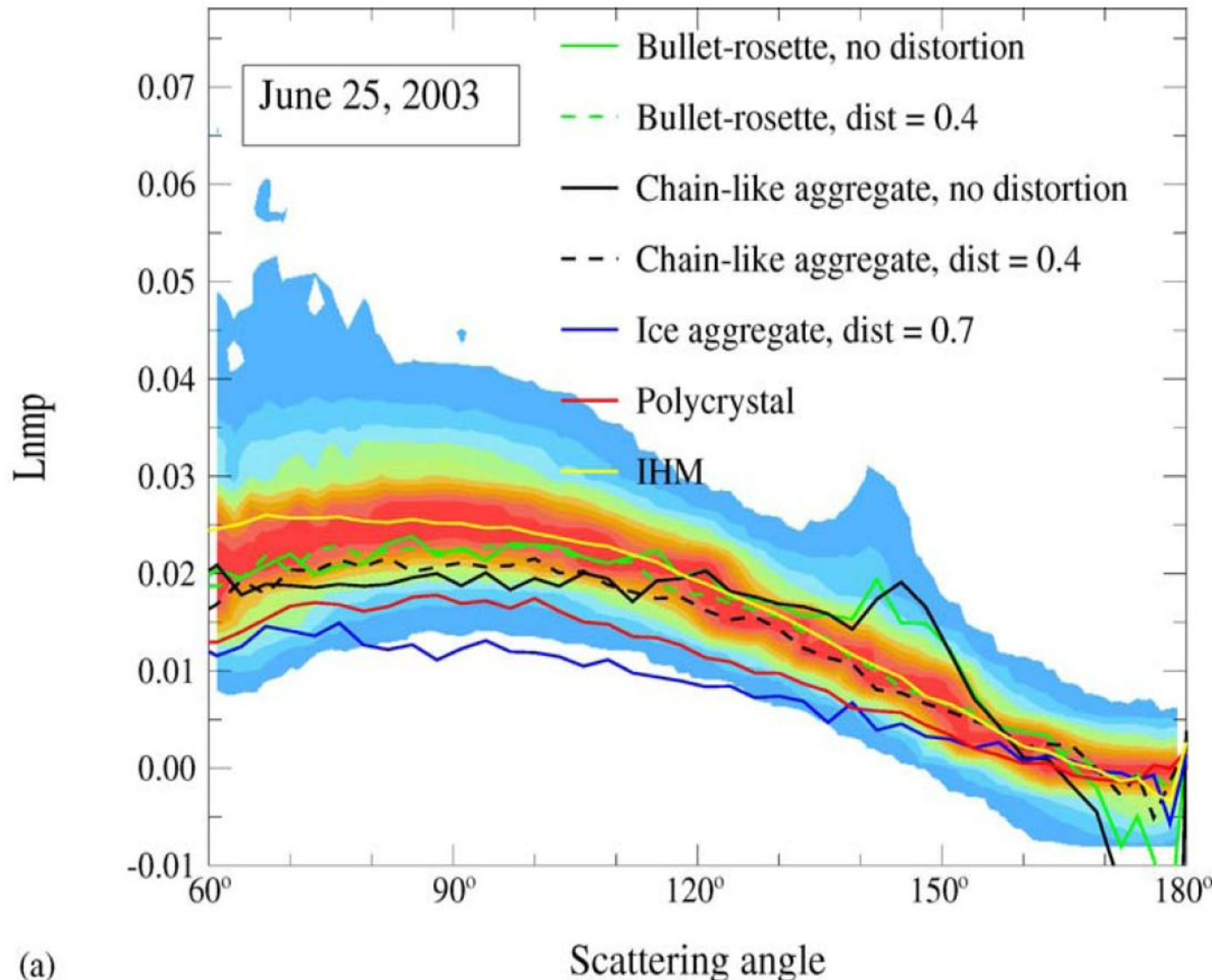
Phase functions of pristine or heterogeneous particles are very different :

- Pristine (smooth) hexagonal particles tend to produce marked angular features in the phase function which remain in observed distribution of angular reflectance
- Features vanish when surfaces are roughened or heterogeneities are introduced.



Ice Cloud Microphysics

Modelled VS observed global mean polarized signature of ice clouds



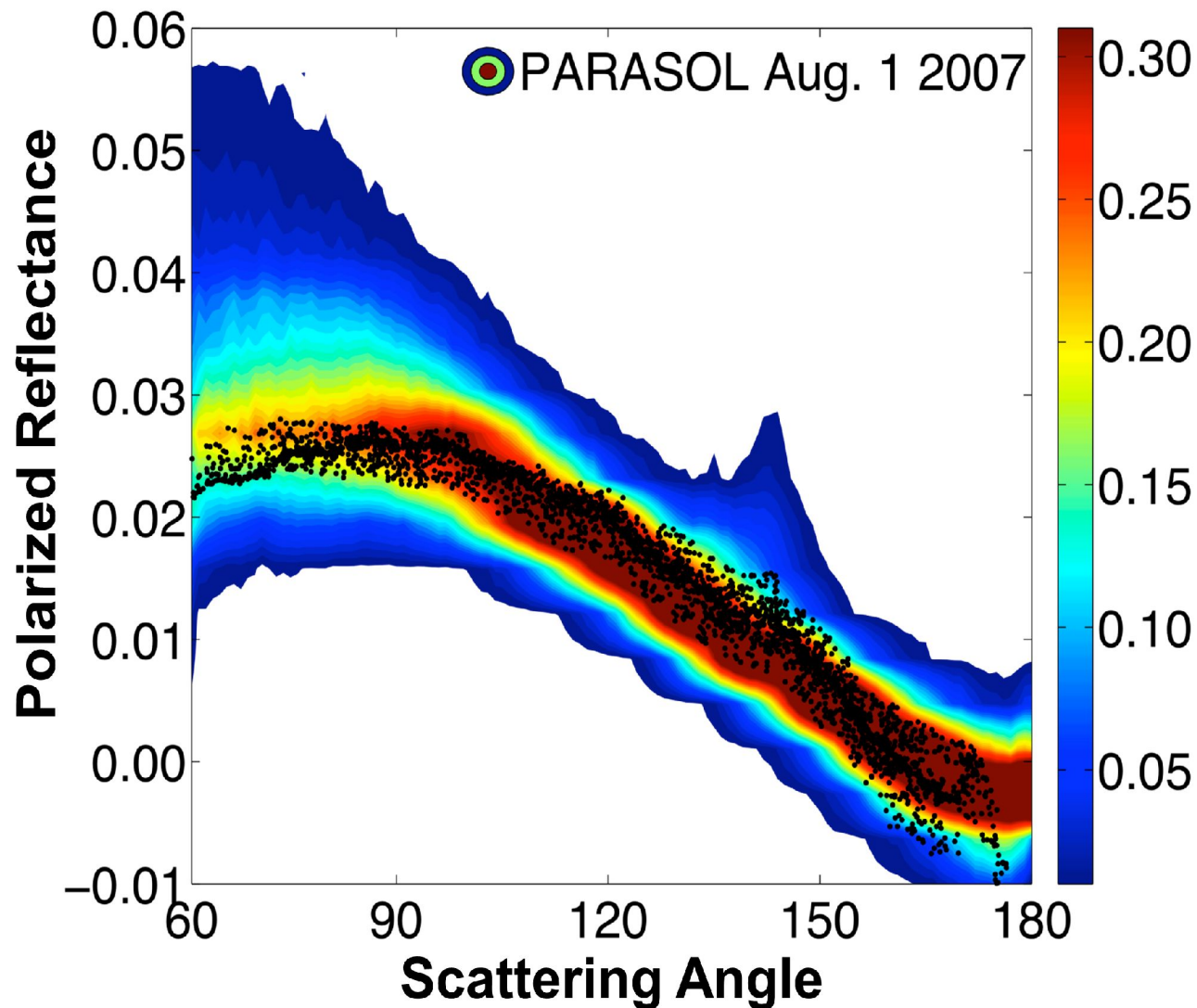
Can also look for a mean equivalent model representative of an average ice cloud.

Labonnote et al (2001) demonstrated the Inhomogeneous Hexagonal Model (IHM) can be used to fit well both total and polarized multiangle reflectances from POLDER.

Figure from : A. J. Baran and L. C-Labonnote, JQSRT (2006)

Ice Cloud Microphysics

Modelled VS observed global mean polarized signature of ice clouds



Polarized reflectances simulated for the “best” combination of the retrieved habits and roughnesses calculated for POLDER data recorded on 1 August 2007.

The polarized reflectances were calculated for the habit and roughness value inferred for each the up-to-16 directions available PARASOL pixel. The effective diameter is 60 micrometers. Color contours are density of PARASOL polarized reflectance observations, and black dots are simulations. Each dot represents a calculation of the resulting polarized reflectance for a single viewing geometry.

Fig 6. from Cole et al, ACPD - 2013

Ice Cloud Microphysics

Further reading

Van Diedenhoven, B., B. Cairns, I.V. Geogdzhayev, A.M. Fridlind, A.S. Ackerman, P. Yang, and B.A. Baum, 2012: Remote sensing of ice crystal asymmetry parameter using multi-directional polarization measurements. Part I: Methodology and evaluation with simulated measurements. *Atmos. Meas. Tech.*, 5, 2361-2374, doi:10.5194/amt-5-2361-2012.

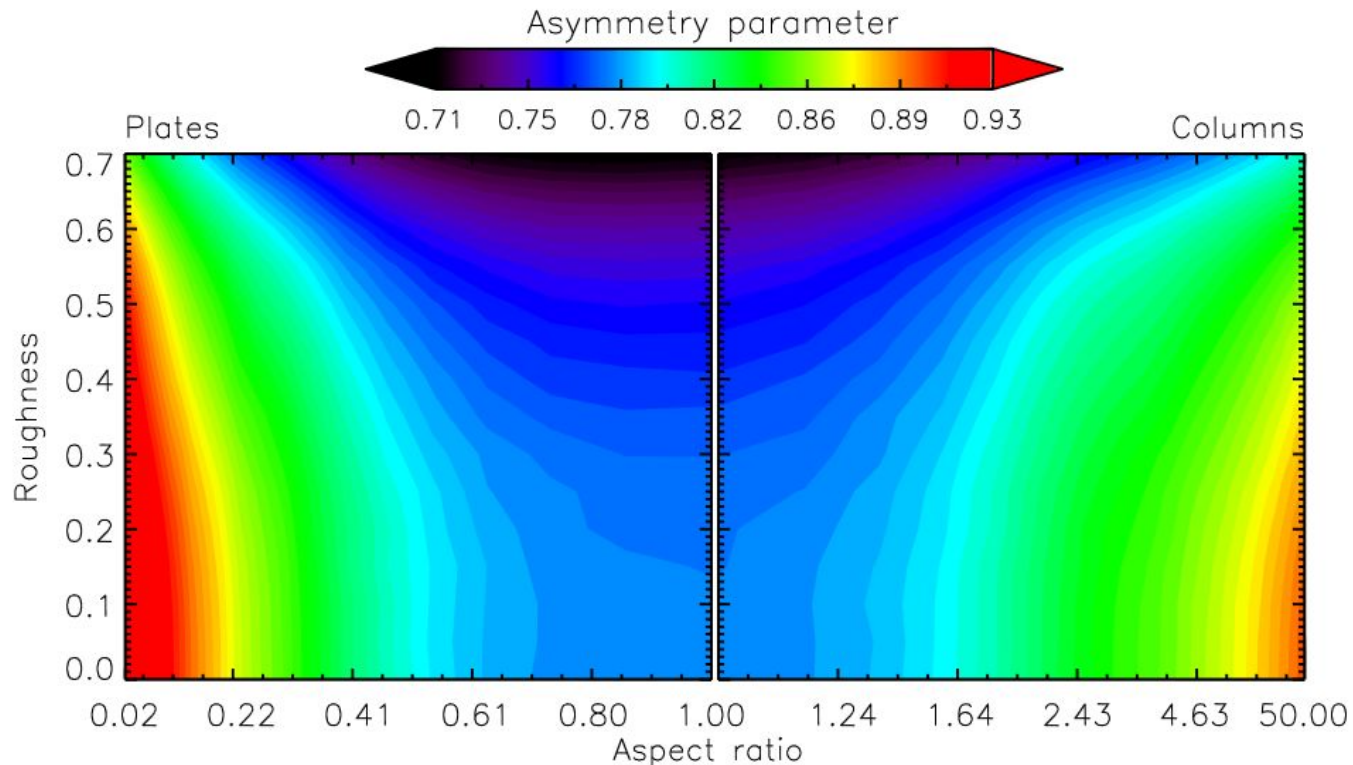
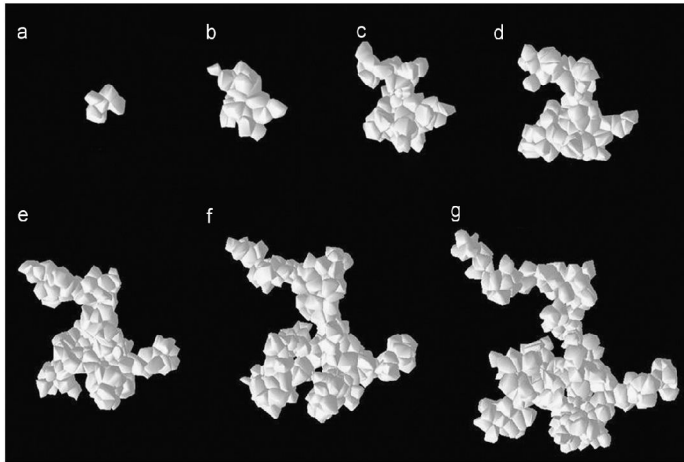


Fig. 1. Asymmetry parameters of plates and columns at 864 nm as a function of their aspect ratio and microscale roughness.

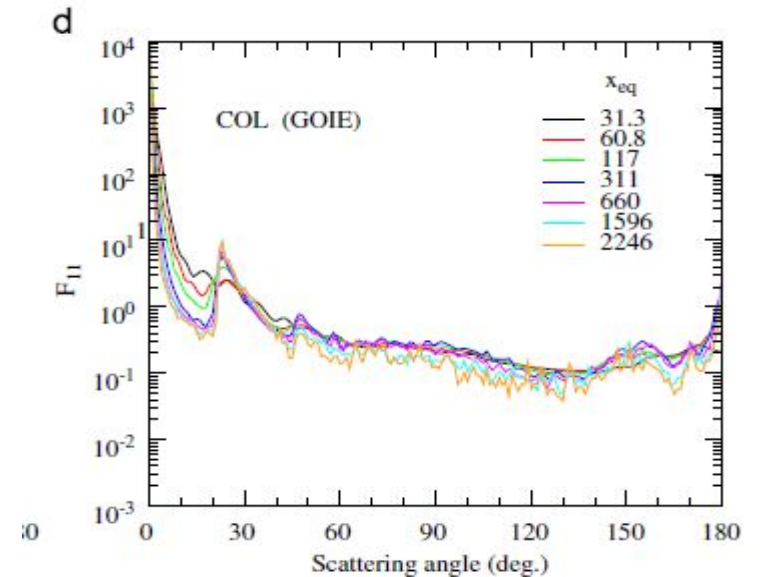
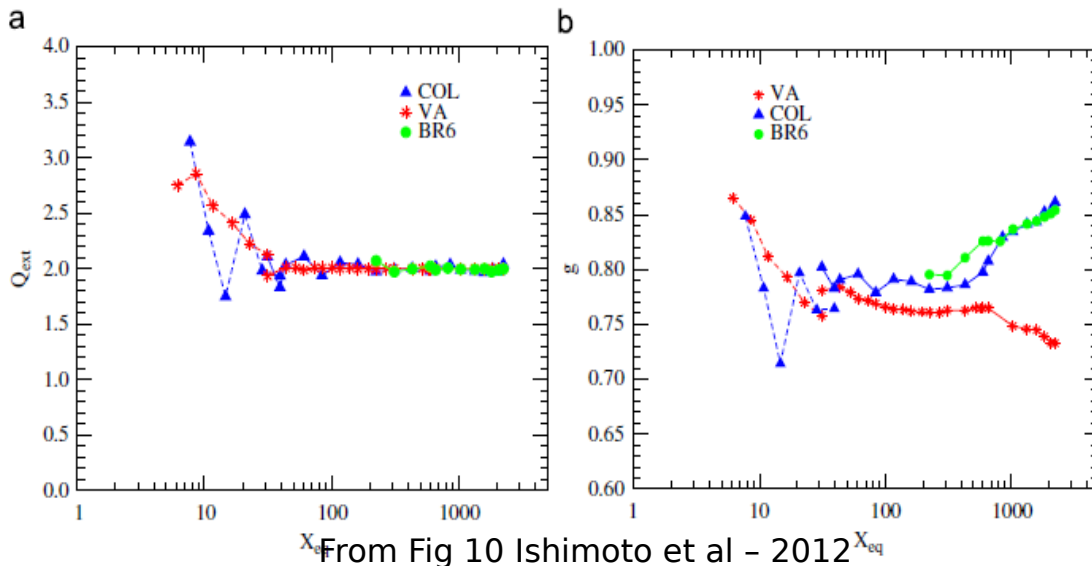
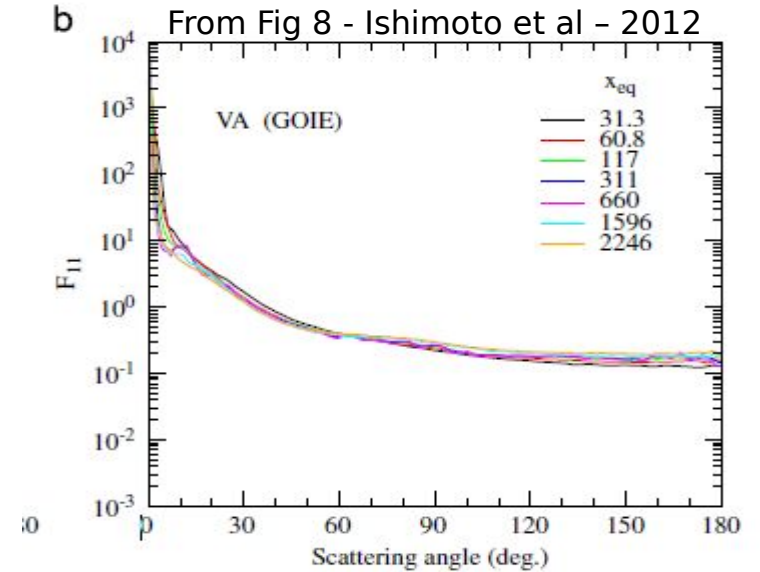
See also application to RSP : Van Diedenhoven, B., B. Cairns, A.M. Fridlind, A.S. Ackerman, and T.J. Garrett, 2013: Remote sensing of ice crystal asymmetry parameter using multi-directional polarization measurements – Part 2: Application to the Research Scanning Polarimeter. *Atmos. Chem. Phys.*, 13, 3185-3203, doi:10.5194/acp-13-3185-2013.

H. Ishimoto, K. Masuda, Y. Mano, N. Orikasa, A. Uchiyama : Irregularly shaped ice aggregates in optical modeling of convectively generated ice clouds Journal of Quantitative Spectroscopy and Radiative Transfer, Volume 113, Issue 8, May 2012, Pages 632-643

H. Letu, T. Y. Nakajima, and T. N. Matsui, "Development of an ice crystal scattering database for the global change observation mission/second generation global imager satellite mission: investigating the refractive index grid system and potential retrieval error," Appl. Opt. 51, 6172-6178 (2012)



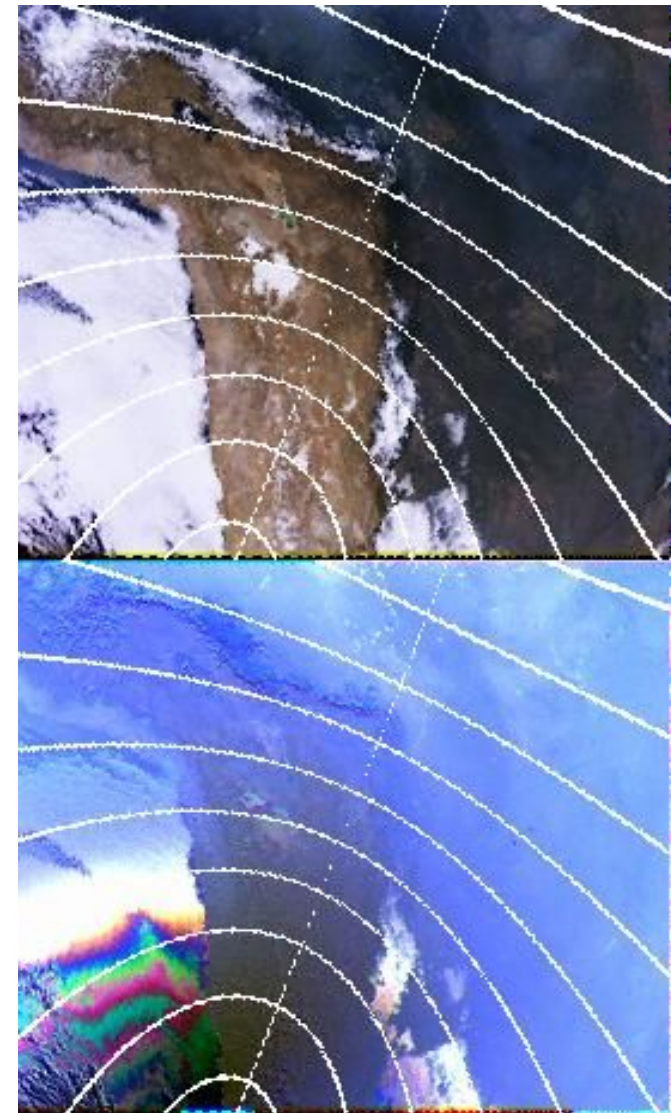
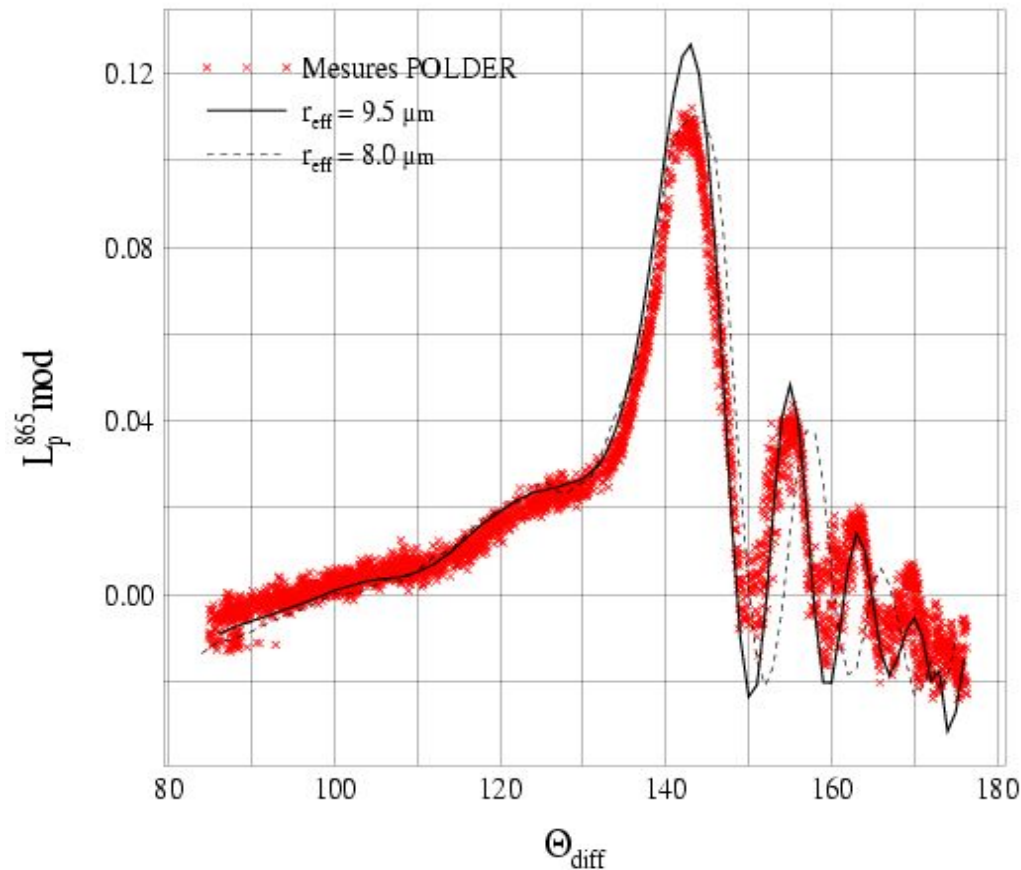
Numerically created Voronoi aggregates for a model of irregular ice particles. (from Ishimoto et al - 2012 - Fig 3.)



Liquid Cloud Droplet Effective Size Distribution

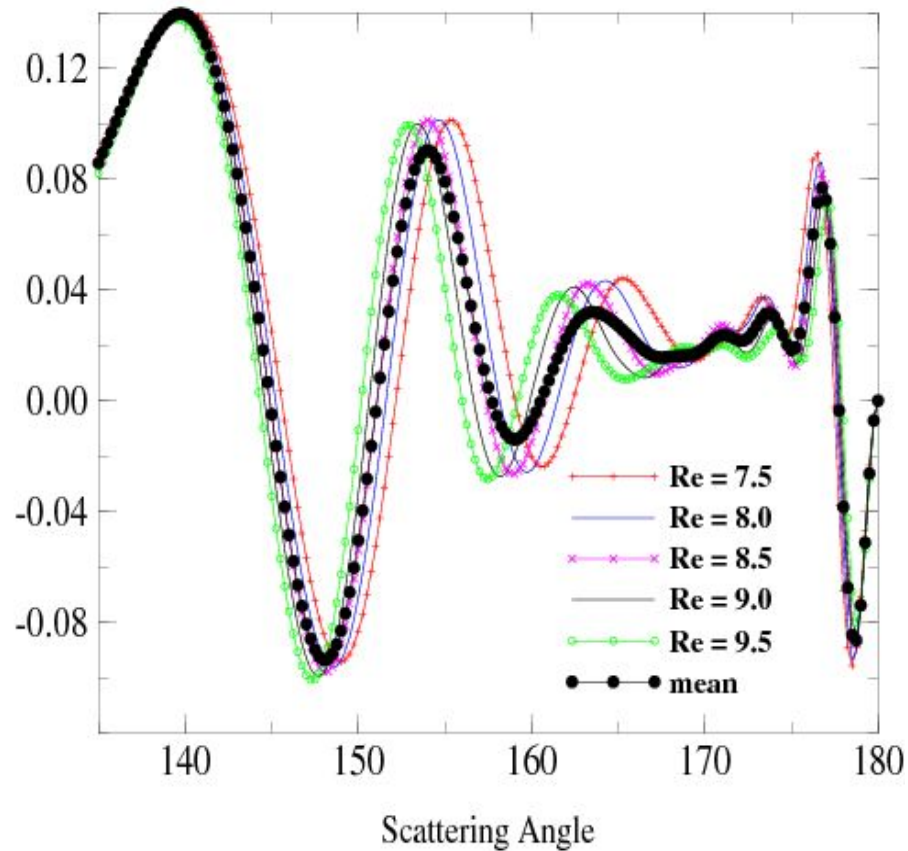
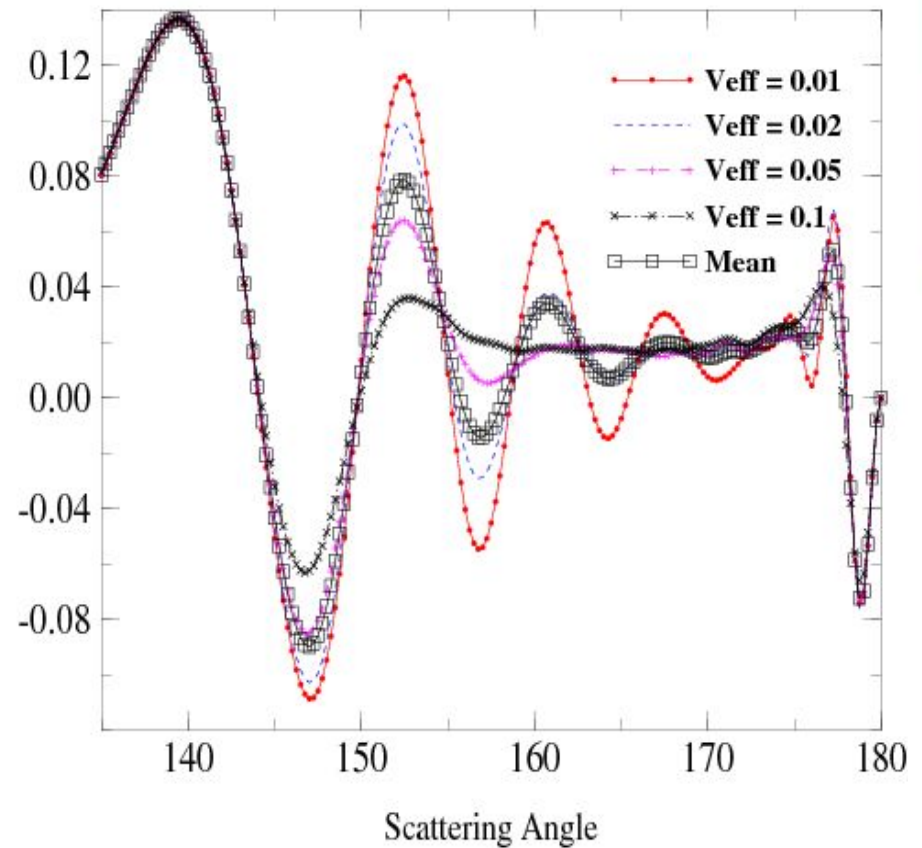
Principle : use of angular features above 140° (supernumerary bows).

Cloud Droplet Distribution : effective radius and variance

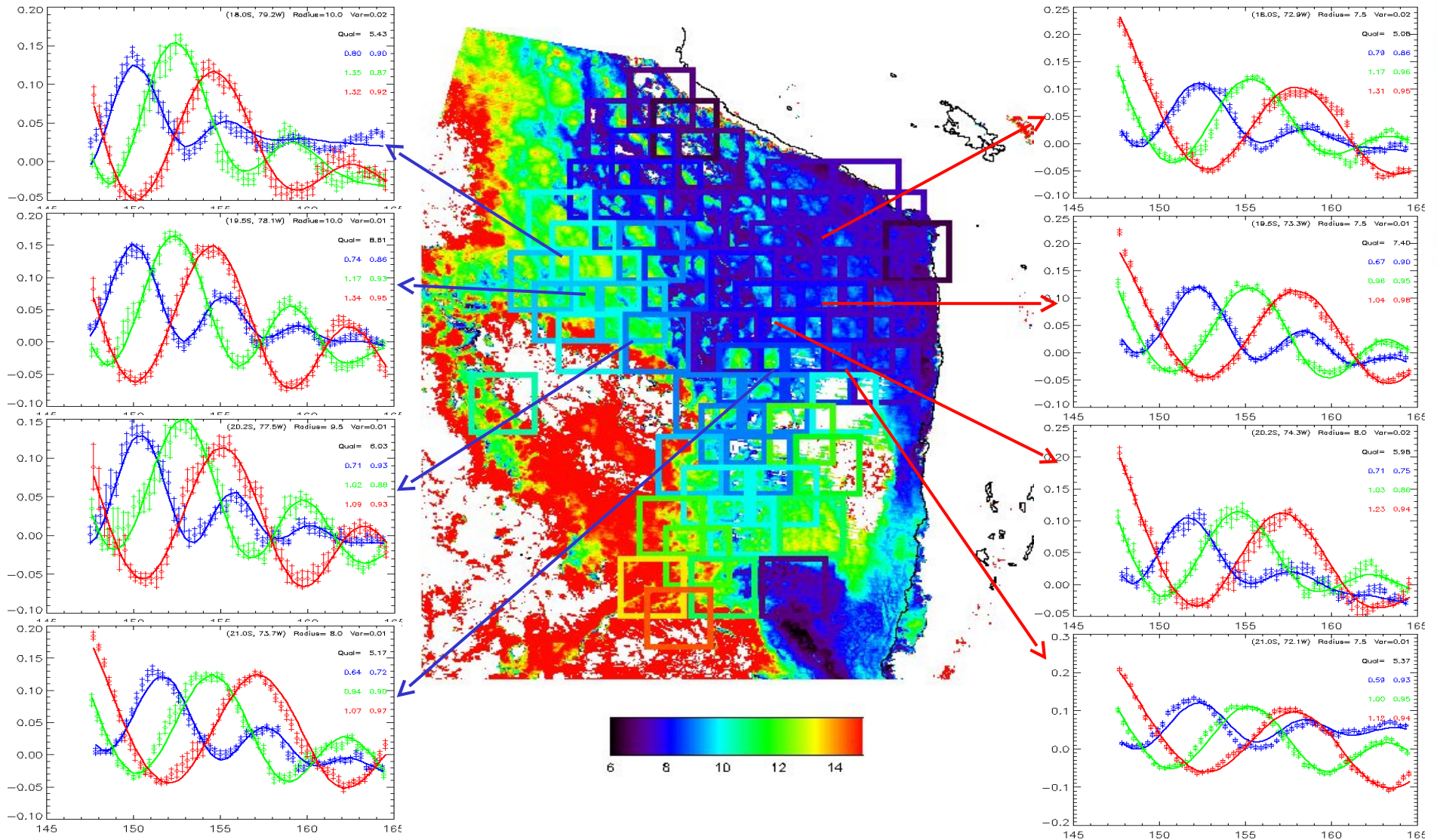


Bréon and Goloub, GRL, (1998)

Polarized phase function for distribution of spherical particles

Constant V_{eff} and varying Re_{eff} Constant Re_{eff} and varying V_{eff}

Liquid Cloud Droplet Effective Size Distribution Comparison with MODIS retrievals

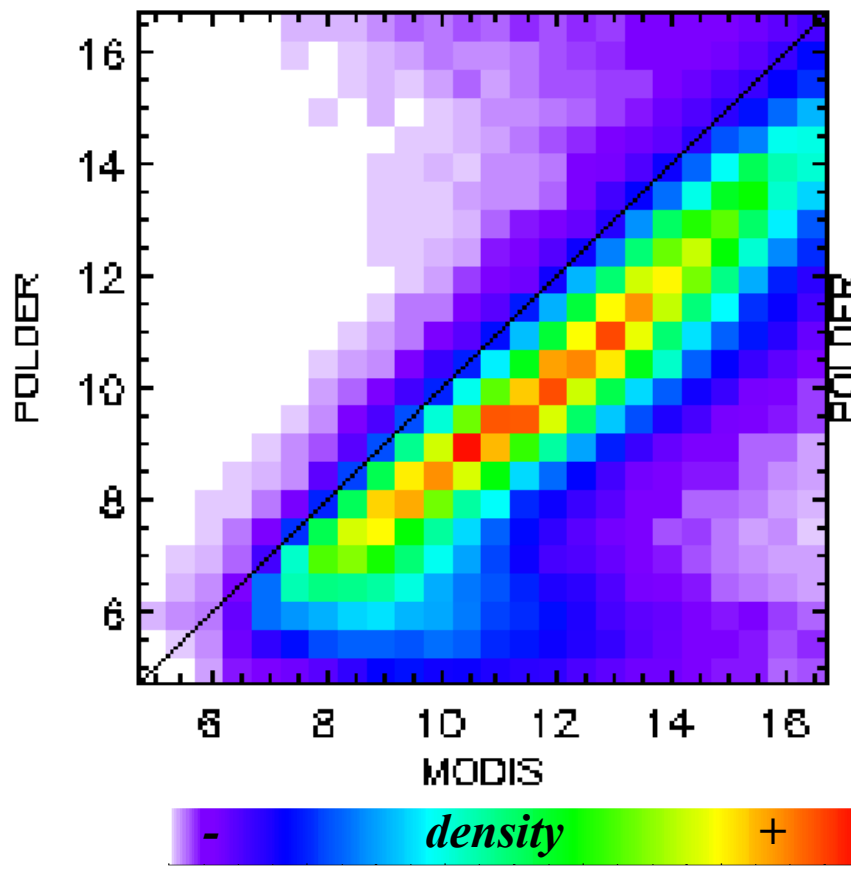


From : Bréon et Doutriaux, JAS (2005)

Liquid Cloud Droplet Effective Size Distribution

Comparison with MODIS retrievals

Comparison between POLDER and MODIS « effective » radii over ocean



Correlation is good but there is an apparent 2 microns bias between POLDER and MODIS retrievals.

POLDER sees smaller droplets than MODIS.

POLDER “less sensitive to biases and errors resulting from cloud heterogeneity, assumptions on the size distribution” when retrieval is possible according to authors.

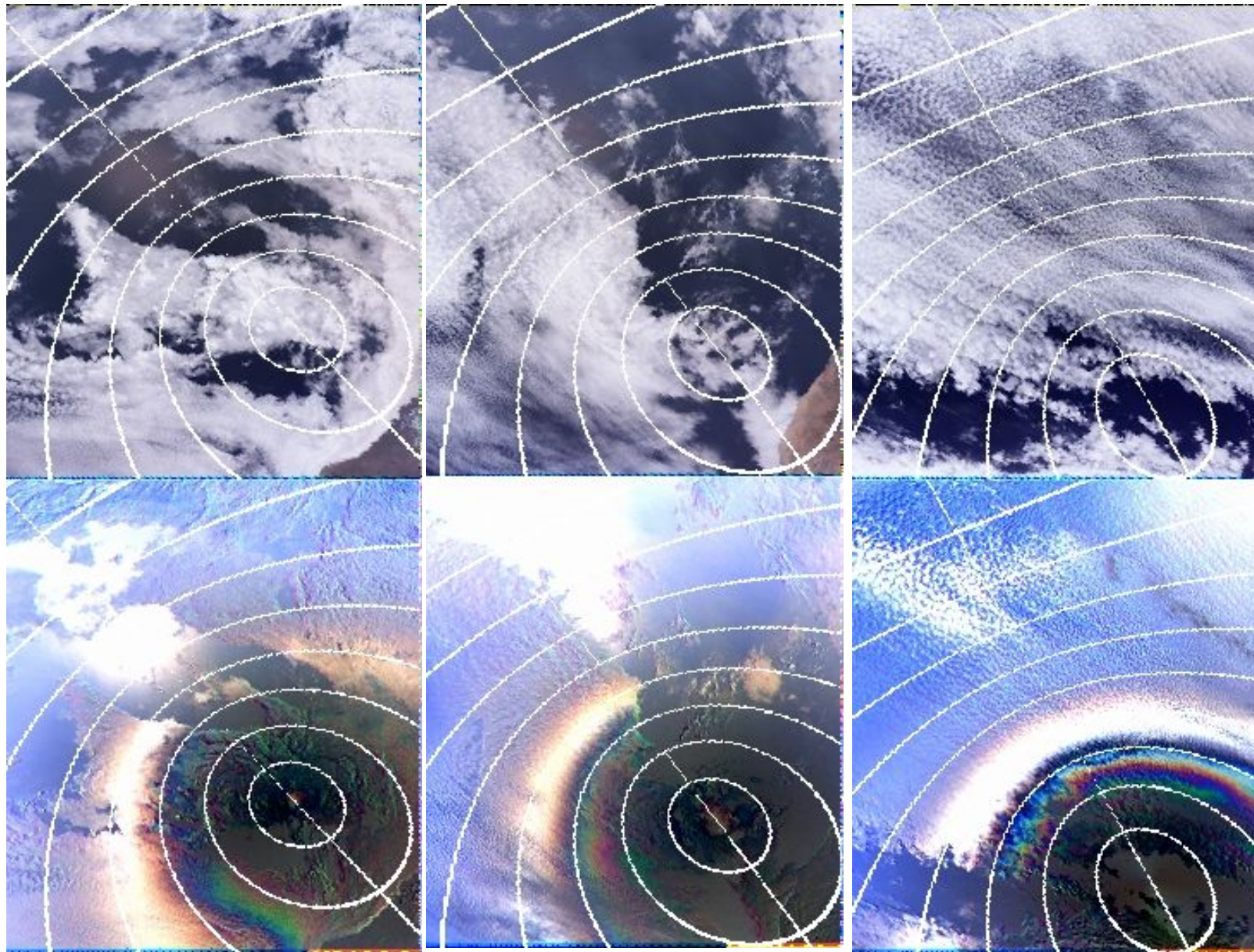
Questions :

Is this real ?

Is one of them correct ? none ? both ?

From : Bréon et Doutriaux, JAS (2005)

About aerosols over cloud



Total
radiance
RGB

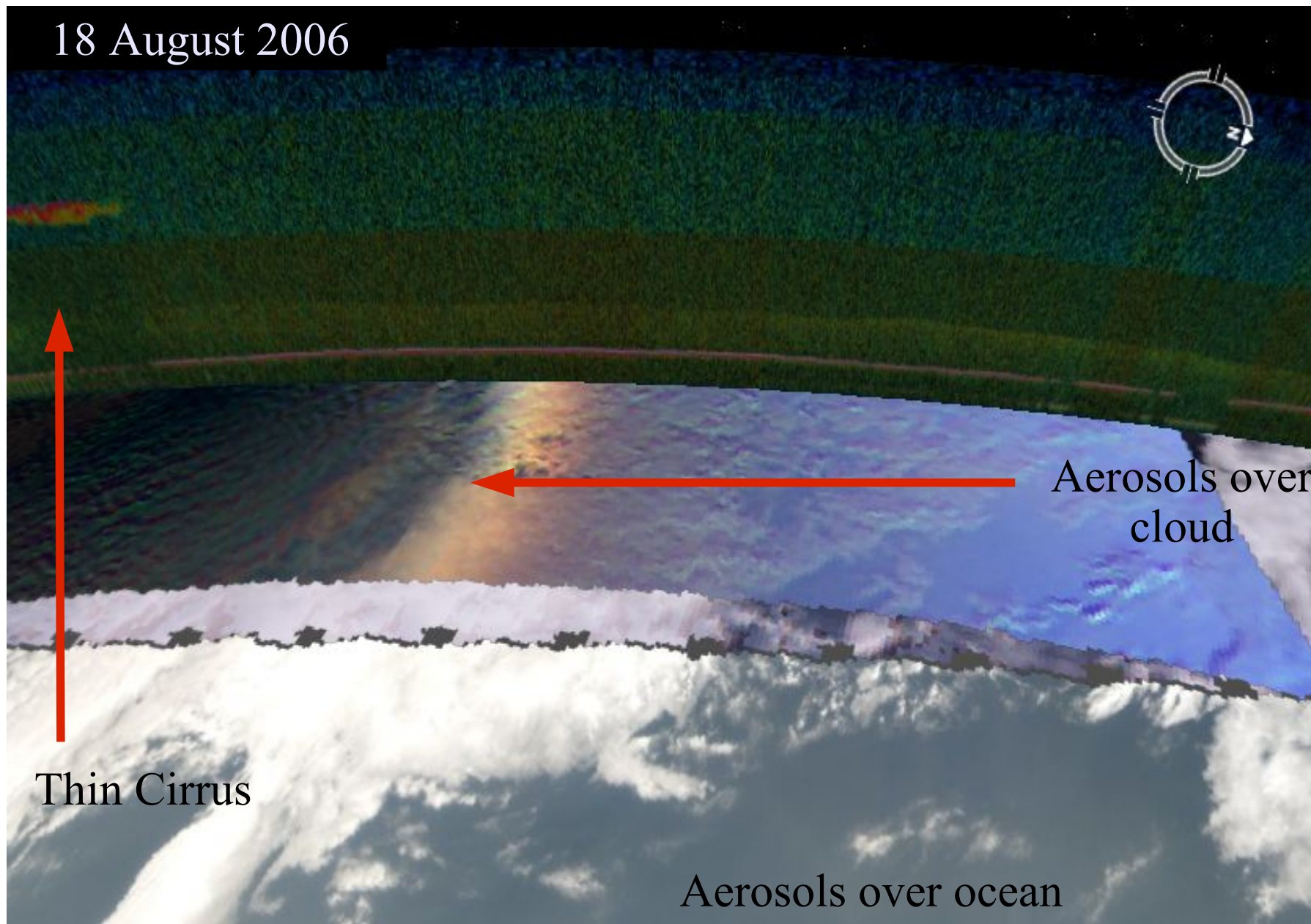
Polarized
radiance
RGB

Polluted

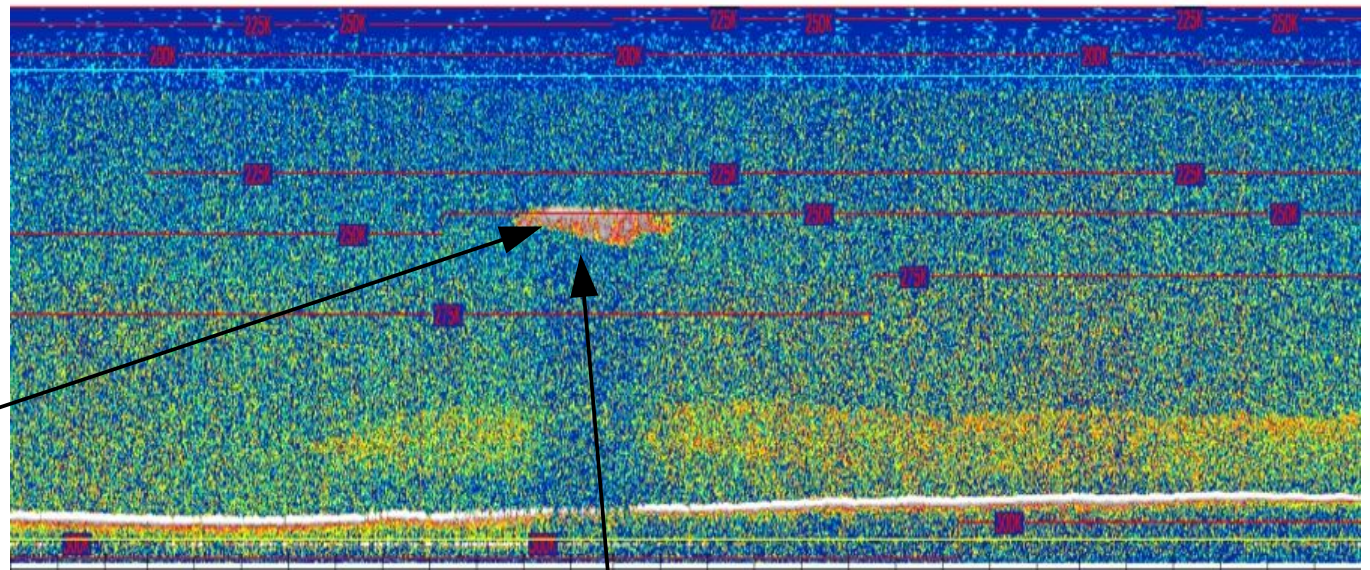
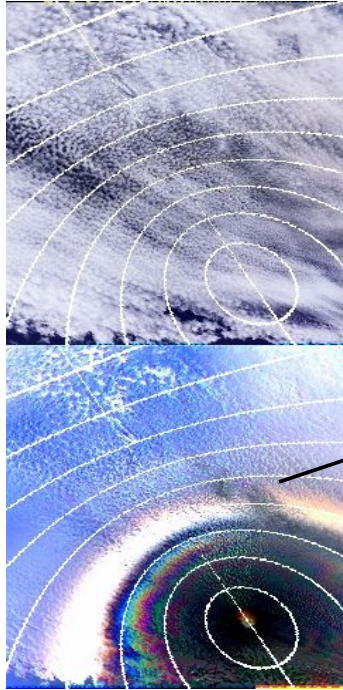
Polluted

Clean

18 August 2006

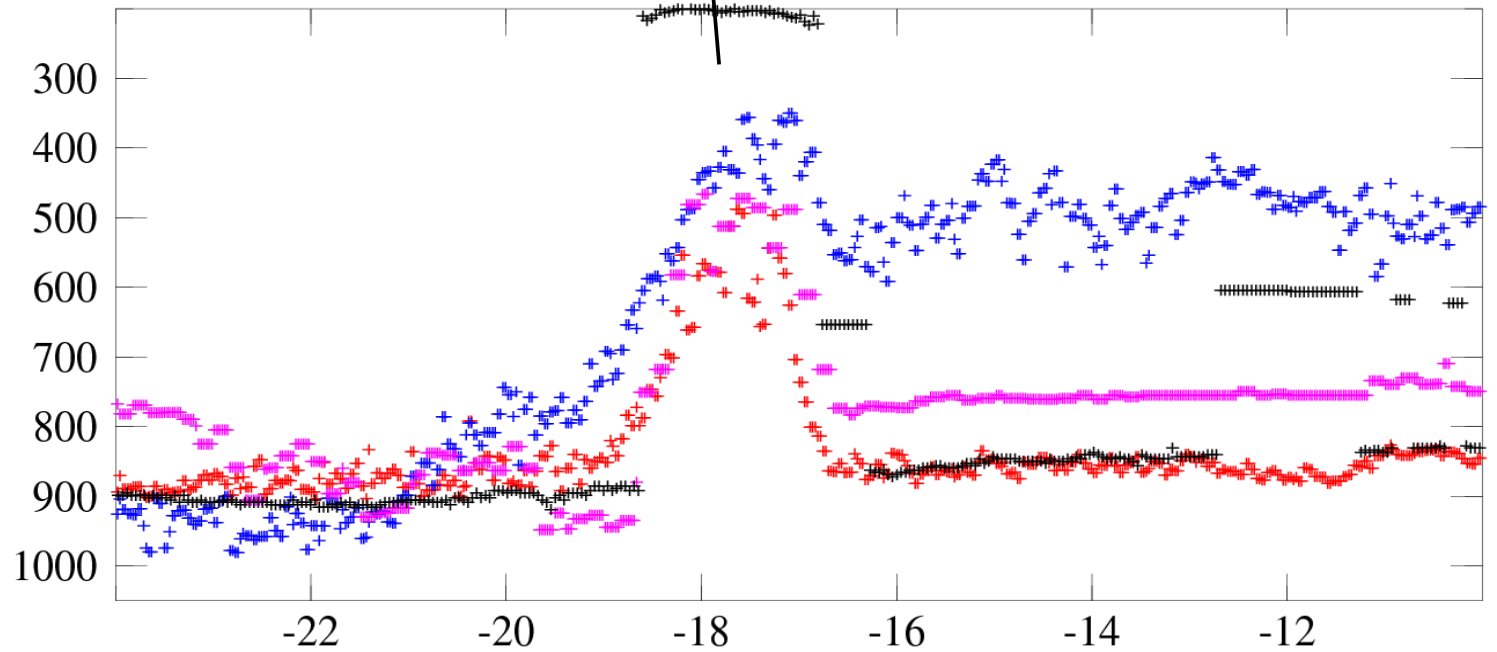


About aerosols over cloud



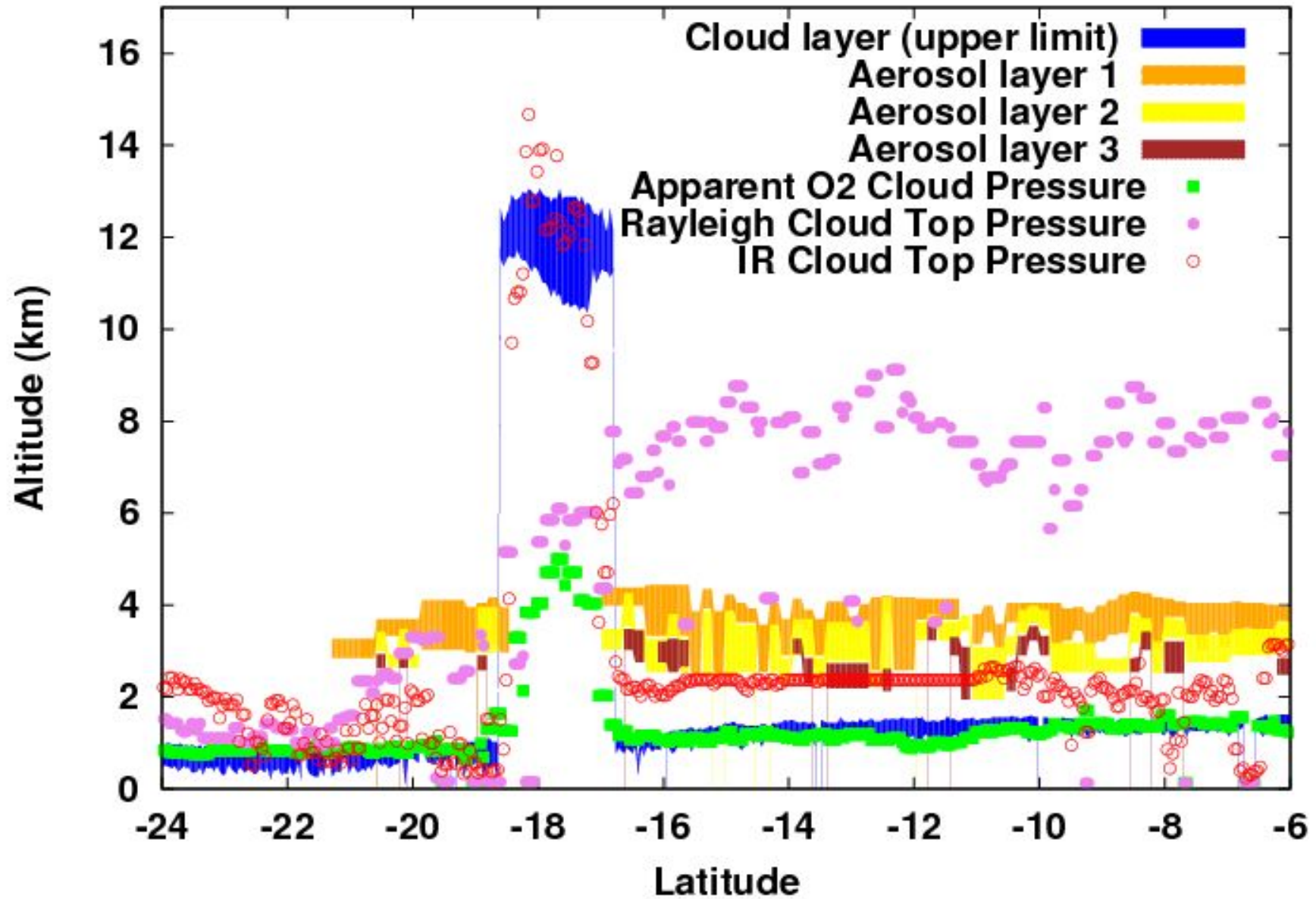
LIDAR*
 O₂
 Rayleigh
 CO₂ / IR

Cloud Top Alt. (hPa)



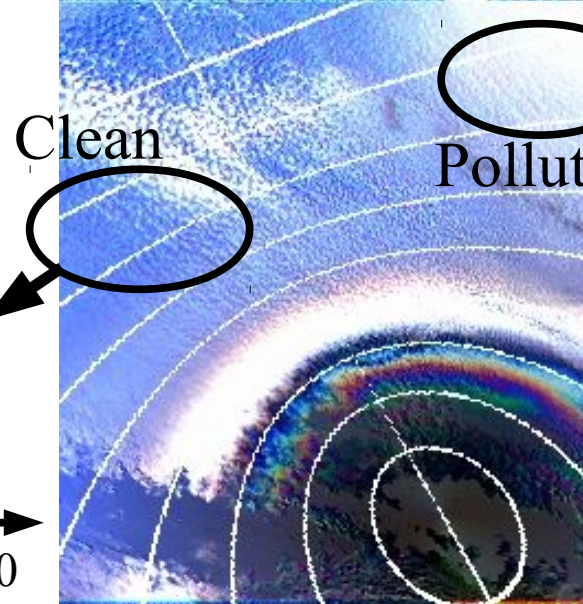
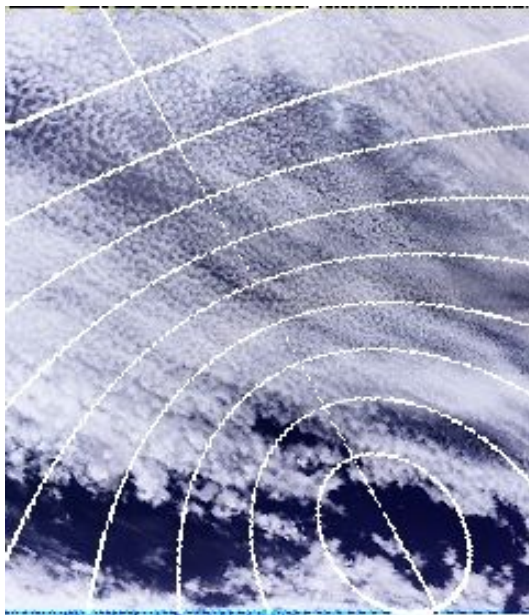
*LIDAR Alt from 5km Cloud Layer product

Latitude



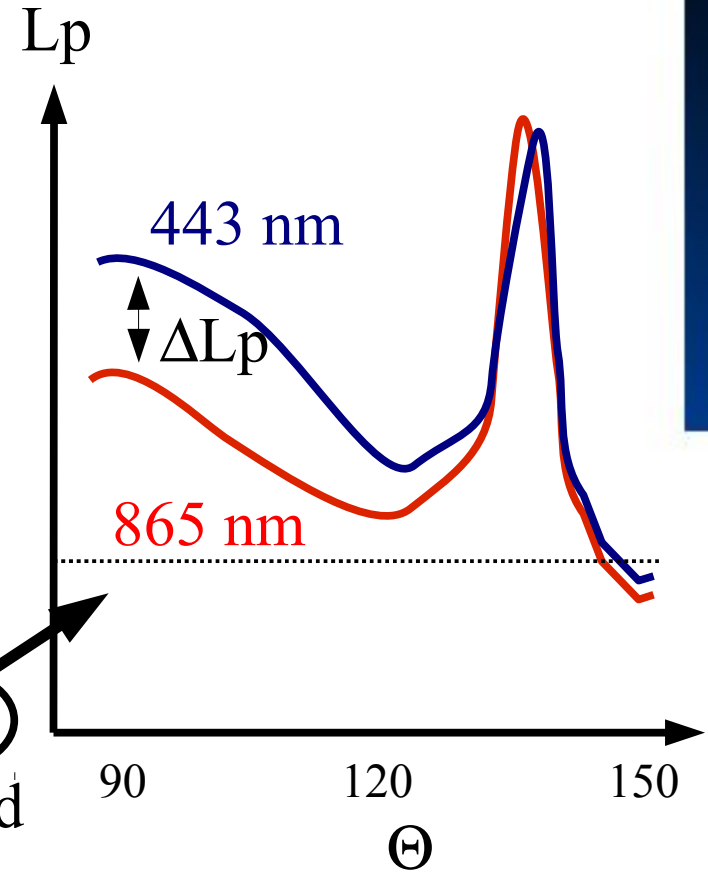
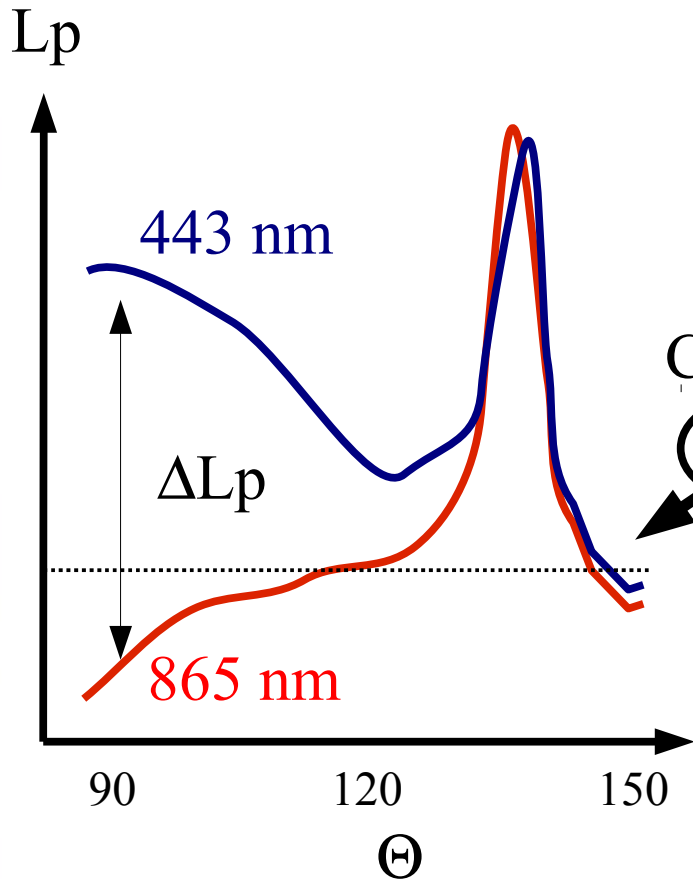
Basis of Rayleigh derived Cloud Top Pressure

Total radiance RGB



Polarized radiance RGB

$$\Delta L_p \sim \tau_{\text{rayleigh}}$$



Signal Modelling of Aerosols over Clouds

Assuming single scattering for aerosol and molecular signal

$$\begin{aligned}
 Lp_{\lambda}(\theta_s, \theta_v, \phi_r) = & \frac{q^m(\Theta) \cdot \tau_{\lambda}^m}{4\mu_v} \\
 & + \frac{\omega_{o,\lambda}^a \cdot q_{\lambda}^a(\Theta) \cdot \tau_{\lambda}^a}{4\mu_v} \cdot \exp[-m\gamma\tau_{\lambda}^m] \\
 & + Lp_{\lambda}^c(\theta_s, \theta_v, \phi_r) \cdot \exp[-m(\gamma\tau_{\lambda}^m + \beta\tau_{\lambda}^a)]
 \end{aligned}$$

Waquet et al (2013) GRL

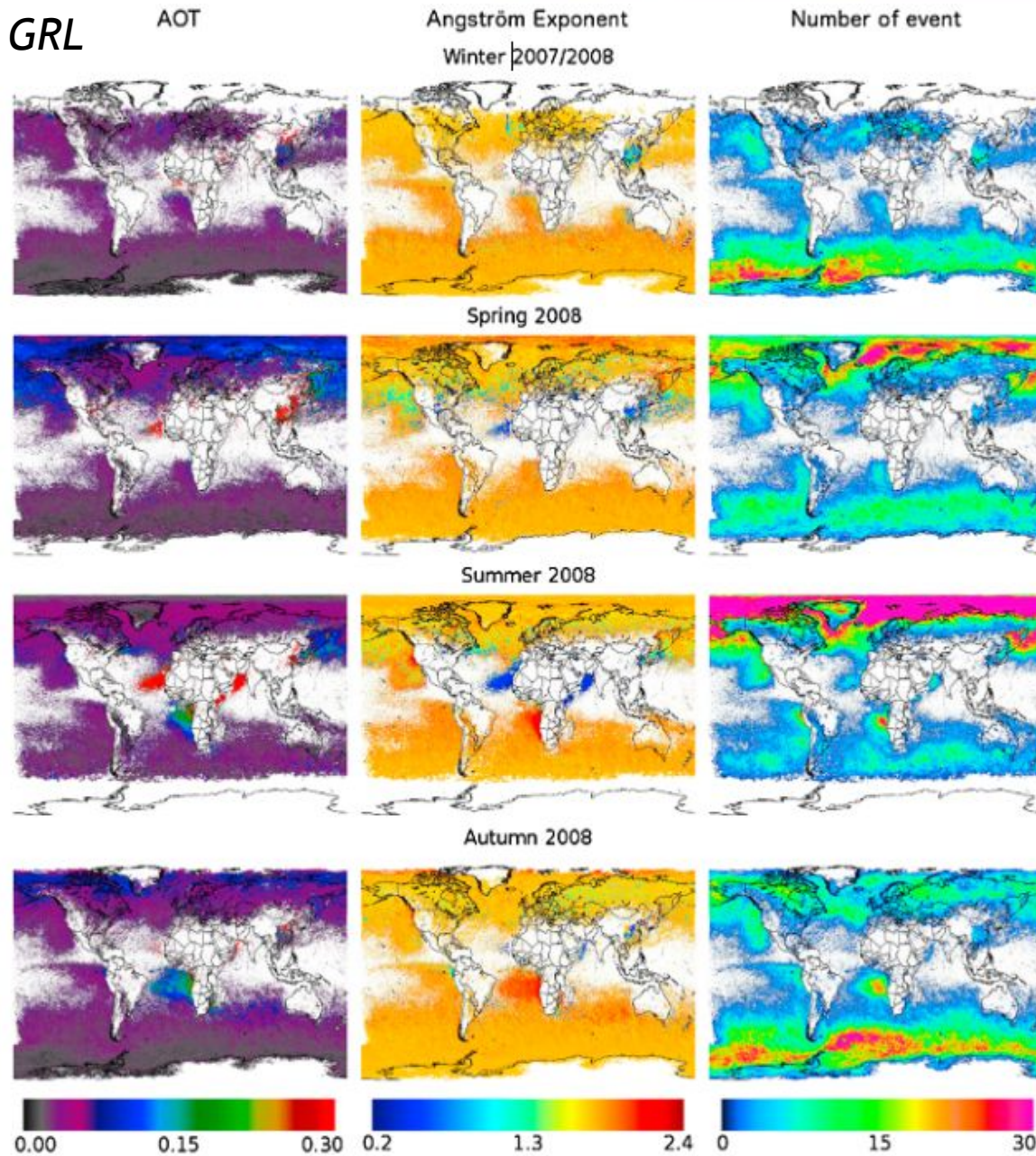


Figure 1. (left column) Global mean aerosol optical thickness at 865 nm, (middle column) mean Ångström exponent retrieved over clouds and (right column) number of retrievals in function of the season.

Further reading about aerosols above clouds

Knobelspiesse, K., Cairns, B., Redemann, J., Bergstrom, R. W., and Stohl, A.: Simultaneous retrieval of aerosol and cloud properties during the MILAGRO field campaign, *Atmos. Chem. Phys.*, 11, 6245-6263, doi:10.5194/acp-11-6245-2011, 2011.

Torres, Omar, Hiren Jethva, P. K. Bhartia, 2012: Retrieval of Aerosol Optical Depth above Clouds from OMI Observations: Sensitivity Analysis and Case Studies. *J. Atmos. Sci.*, 69, 1037-1053.

Waquet, F., Peers, F., Goloub, P., Ducos, F., Thieuleux, F., Derimian, Y., Riedi, J., and Tanré, D.: Retrieval of the Eyjafjallajökull volcanic aerosol optical and microphysical properties from POLDER/PARASOL measurements, *Atmos. Chem. Phys. Discuss.*, 13, 8663-8699, doi:10.5194/acpd-13-8663-2013, 2013.

Waquet, F., F. Peers, F. Ducos, P. Goloub, S. Platnick, J. Riedi, D. Tanré, and F. Thieuleux (2013), Global analysis of aerosol properties above clouds, *Geophys. Res. Lett.*, 40, 5809-5814, doi:10.1002/2013GL057482.

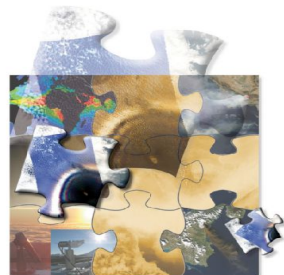
What's next ?



3MI on Eumetsat Polar System - SG

- EPS-SG : a follow-on to current EUMETSAT Polar System (EPS) 2020-2040 timeframe
- Contribute to the Joint Polar System being jointly set up with NOAA
- Two-satellite configuration: Metop-SG-A and -B flying in the same orbit, separated by 180°
- Metop-like orbit: sun synchronous
low earth orbit at 832 km mean altitude
09:30 local time of the descending node
- More information:
<http://www.eumetsat.int/Home/Main/Satellites/EPS-SG>

The **3MI** mission
for operational monitoring
of aerosols from EPS-SG



3MI implementation in a nutshell

Instrument current specifications based on POLDER heritage :
Large field of view 2D Push-broom radiometer (2200 km swath, 4 km pixel at nadir)

Provide images of the Earth TOA outgoing radiance using:

- Multi-view (10 to 14 views; angular sampling in the order of 10°)
- Multi-channel (12 channels from 410 to 2130 nm)
- Multi-polarisation (9 channels with -60° , 0° , $+60^\circ$ polarisers)

Requirements :

- Polarization sensitivity $> 96\%$ for polarized channels
- Polarization sensitivity $< 5\%$ for non polarized channels
- Bandwidth from 10 nm (UV) to 40 nm (SWIR)
- co-registration of ~ 7 sec max between all channels for one direction

3MI implementation in a nutshell

Optical Head	Wavelength [nm]	FWHM [nm]	Polar.	Primary Use
VIS/NIR	410	20	Y	Absorbing aerosol and ash cloud monitoring
	443	20	Y	Aerosols absorption and height indicators
	490	20	Y	Aerosol, surface albedo, cloud reflectance, cloud optical depth
	555	20	Y	Surface albedo
	670	20	Y	Aerosols properties
	763	10	N	Cloud and aerosols height
	765	40	N	Cloud and aerosols height
	865	40	Y	Vegetation, aerosol, clouds, surface features
SWIR	910 VIS/NIR	20	N	Water vapour , atmospheric correction
	910 SWIR	20	N	Water vapour , atmospheric correction
	1370	40	Y	Cirrus clouds, water vapour imagery
	1650	40	Y	Ground characterisation for aerosol inversion
	2150	40	Y	Ground characterisation for aerosol inversion, Cloud microphysics at cloud top, Vegetation, fire (effects)

Final take home question:

Polarisation is that small missing piece in your remote-sensing puzzle →



Can you really afford not to have it ?